A NONITERATIVE RECONSTRUCTION METHOD FOR THE INVERSE POTENTIAL PROBLEM WITH PARTIAL BOUNDARY MEASUREMENTS

L. FERNANDEZ, A.A. NOVOTNY, AND R. PRAKASH

ABSTRACT. In this paper, a noniterative reconstruction method for solving the inverse potential problem is proposed. The forward problem is governed by a modified Helmholtz equation. The inverse problem consists in the reconstruction of a set of anomalies embedded into a geometrical domain from partial or total boundary measurements of the associated potential. Since the inverse problem is written in the form of an ill-posed boundary value problem, the idea is to rewrite it as a topology optimization problem. In particular, a shape functional measuring the misfit between the solution obtained from the model and the data taken from the boundary measurements is minimized with respect to a set of ball-shaped anomalies by using the concept of topological derivatives. It means that the shape functional is expanded asymptotically and then truncated up to the desired order term. The resulting truncated expansion is trivially minimized with respect to the parameters under consideration which leads to a noniterative second order reconstruction algorithm. As a result, the reconstruction process becomes very robust with respect to the noisy data and independent of any initial guess. Finally, some numerical experiments are presented showing the capability of the proposed method in reconstructing multiple anomalies of different sizes and shapes by taking into account complete or partial boundary measurements.

1. INTRODUCTION

The topological derivative [37] represents the first term of the asymptotic expansion of a given shape functional with respect to a small parameter which measures the size of singular domain perturbations, such as holes, inclusions, source-terms and cracks. This relatively new concept has been successfully applied in many different fields [34], including shape and topology optimization, inverse problems, image processing, multiscale material design and mechanical modeling involving damage and fracture evolution phenomena. The topological derivative can be seen as a particular case of the broader class of asymptotic methods fully developed in the books by Ammari & Kang [4] and Ammari et al. [2], for instance.

In particular, the topological derivative has been successfully applied for solving a wide class of inverse problems. The basic idea consists in minimizing a shape functional measuring the misfit between boundary measurements and the solution obtained from the model by using the topological derivative. The obtained sensitivity depending on the background solution gives qualitative information on the shape and topology of hidden defects. Actually, the topological derivative with respect to the nucleation of a small crack embedded into a membrane has been applied in the context of fracture detection from boundary measurements of the associated potential [6]. In addition, topological derivative has also

Key words and phrases. Inverse potential problem, modified Helmholtz equation, higher-order topological derivatives, topology optimization, reconstruction method.

been used to determine the location of small cavities in Stokes flow from velocity boundary measurements [1]. Special attention has been devoted to the topological derivative associated with the Helmholtz problem [36], which has been successfully applied for imaging small acoustic anomalies [5, 14, 18, 22, 23, 30]. See also an experimental validation of the topological derivative method in the context of elastic-wave imaging [38]. The stability and resolution analysis for a topological-derivative-based imaging functional has been presented in [3], showing why it works so well in the context of inverse scattering. See also the related work [24]. Finally, applications of topological derivatives in the context of time domain inverse scattering problem can be found in [8, 15, 17], for instance.

More recently, some reconstruction problems have been solved with the help of higher order topological derivatives [26]. In particular, the shape functional governing the inverse problem is expanded asymptotically with respect to a set of ball-shaped anomalies and then truncated up to some desired order term. The resulting expression is trivially minimized with respect to the parameters under consideration, leading to a noniterative second-order reconstruction algorithm. As a result, the stability issues found in most of the inverse problems has been resolved naturally in the current analysis. In particular, the reconstruction process becomes very robust with respect to the noisy data and also independent of any initial guess. See, for instance [12, 13, 21, 33, 35]. Iterative reconstruction algorithms based on level-set methods, for instance, are widely used for solving a large class of inverse reconstruction problems [11, 16, 28]. In contrast to the methods based on the topological derivative concept, level-set-based methods are dependent on the initial guess and, in general, the reconstruction process requires a high number of iterations.

Following the original ideas presented in [19, 20], in this paper we are interested in the open problem [27, pp. 126, Problem 4.2], whose physical motivation comes out from semiconductors theory. See also the book [31]. In particular, the corresponding forward problem is governed by a modified Helmholtz equation into two spatial dimensions. The inverse problem under consideration is about the reconstruction of a set of anomalies embedded in a geometrical domain with the help of total or partial measurements of the associated potential on its boundary. More precisely, let $\Omega \subset \mathbb{R}^2$ be an open and bounded domain with smooth boundary $\partial\Omega$ and $\Gamma_\circ \subseteq \partial\Omega$ be the part of the boundary where the measurements of a scalar field of interest are taken. As illustrated in Figure 1(a), there may be an unknown number ($N^* \in \mathbb{Z}^+$) of isolated anomalies ω_i^* within the domain Ω, i.e., there is a set $\omega^* = \cup_{i=1}^{N^*} \omega_i^*$, with open connected components ω_i^* which satisfy $\overline{\omega_i^*} \cap \overline{\omega_j^*} = \emptyset$ for $i \neq j$ and $\overline{\omega_i^*} \cap \partial\Omega = \emptyset$ for each $i, j \in \{1, \cdots, N^*\}$.

We consider the domain Ω as a bounded region representing a fluid medium which contains a different fluid substance within a subdomain ω^*. For a given flux g_N imposed on $\partial\Omega$, the resulting substance concentration (potential) z in Ω is observed on a part of the boundary $\Gamma_\circ \subseteq \partial\Omega$. In this set up, the inverse problem consists in finding k_{ω^*} such that the substance concentration z satisfies the following over-determined boundary value problem

$$\left\{ \begin{array}{rcll} -\Delta z + k_{\omega^*} z & = & 0 & \text{in} \quad \Omega, \\ \partial_n z & = & g_N & \text{on} \quad \partial\Omega, \\ z & = & g_D & \text{on} \quad \Gamma_\circ, \end{array} \right. \tag{1.1}$$

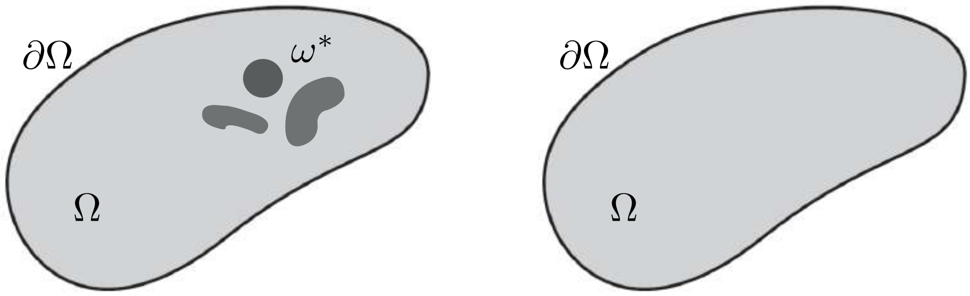

(a) (b)

FIGURE 1. A domain Ω (a) with a set of anomalies ω^* and (b) without anomalies.

where g_N and g_D are the boundary excitation and boundary measurement, respectively. The parameter k_{ω^*} is defined as

$$k_{\omega^*} = \begin{cases} k & \text{in } \Omega \setminus \overline{\omega^*}, \\ \gamma_i k & \text{in } \omega_i^*, \; i = 1, \cdots, N^*, \end{cases} \tag{1.2}$$

with $k, \gamma_i \in \mathbb{R}^+$, where γ_i is the contrast with respect to the material property of the background k. Therefore, in comparison to [19, 20], the main novelty of the current article is the consideration of a contrast on the material properties in place of compact supported anomalies. This drives us to choose completely different adjoint and auxiliary states whose analysis leaded us to use the Bessel's functions of different types. Another vital aspect of this paper, in comparison to [19, 20], is the collection of partial data on the boundary of the domain which makes the inverse problem much more difficult and the obtained result far more relevant from the application point of view but produced the requirement to devise a completely different computational mechanism.

Now, for an initial guess k_ω of k_{ω^*}, we consider the substance concentration field u to be the solution to the boundary value problem

$$\begin{cases} -\Delta u + k_\omega u = 0 & \text{in } \Omega, \\ \partial_n u = g_N & \text{on } \partial\Omega, \end{cases} \tag{1.3}$$

where

$$k_\omega = \begin{cases} k & \text{in } \Omega \setminus \overline{\omega}, \\ \gamma_i k & \text{in } \omega_i, \; i = 1, \cdots, N. \end{cases} \tag{1.4}$$

The quantity k_{ω^*} is unknown and hence z but we assume that z can be measured in $\Gamma_\circ$. Therefore, we would like to find k_{ω^*} with the help of measurements of z taken in $\Gamma_\circ$. If we want to look for an appropriate k_{ω^*}, we wish u to agree with z in $\Gamma_\circ$ i.e. we want $u = z_{|\Gamma_\circ}$. In addition, it is well known that we can not reconstruct both the support ω_i^* and the associated contrast γ_i simultaneously. It comes out from the lack of uniqueness when both parameters are unknown [19, 20]. Therefore, we assume that γ_i, $i = 1, \cdots, N^*$ are given and then we focus on the reconstruction of their supports ω_i^*, $i = 1, \cdots, N^*$ from total or partial boundary measurements taken on $\partial\Omega$.

Since the inverse problem (1.1) is written in the form an ill-posed and over-determined boundary value problem, the idea is to rewrite it as a topology optimization problem [32], namely

$$\underset{\omega \subset \Omega}{\text{Minimize}} \ \mathcal{J}_\omega(u^1, \cdots, u^M) = \sum_{m=1}^{M} \int_{\Gamma_\circ} (u^m - z^m)^2 \,, \tag{1.5}$$

where $M \in \mathbb{Z}^+$ is the number of observations, z^m and u^m are the solutions of the boundary value problems (1.1) and (1.3), respectively, corresponding to the Neumann data g_N^m with $m = 1, \cdots, M$. Notice that, the minimizer of the topology optimization problem (1.5) produces the best approximation to ω^*, solution of the inverse problem (1.1), in an appropriate sense.

The outline of this paper is as follows. In Section 2, we present some preliminaries including the definitions of first-order and higher-order topological derivatives as well as the series expansions of some Bessel functions that will be used to establish our main result. Since the inverse problem we are dealing with is rewritten as a topology optimization problem, we introduce in Section 3 some tools from the asymptotic methods based on the topological derivative concept, namely, the functionals associated to the unperturbed and perturbed domains, the *ansätz* for a scalar field of interest and some auxiliary boundary value problems. The topological asymptotic expansion of the shape functional is presented in Section 4, which is the main result of this article. The *a priori* estimates of the remainders, obtained in Section 4, are presented in Appendix A. The resulting reconstruction algorithm is described in Section 5. In order to investigate the capability of the proposed method in reconstructing multiple anomalies of different sizes and shapes, some numerical experiments are presented in Section 6. We consider complete and partial boundary measurements and test the robustness of the reconstruction algorithm with respect to noisy data. Finally, the paper ends in Section 7 with some concluding remarks.

2. Preliminaries

Since the inverse problem (1.1) is rewritten as the topology optimization problem (1.5), we seek to solve the optimization problem by using the concept of topological derivative which has been successfully applied to solve a number of inverse problems. In fact, the concept of topological derivative has been used to devise different numerical schemes for solving the EIT [9, 21, 26], gravimetry [12, 13], among others anomalies detection problems [19, 35]. Therefore, for the sake of completeness of the manuscript, we briefly present in Section 2.1 the main definitions of topological derivatives. Next, in Section 2.2, we introduce series expansions of some Bessel functions that will be used in further calculations.

2.1. **Topological derivatives.** The topological derivative measures the sensitivity of a given shape functional with respect to infinitesimal singular domain perturbations such as the insertion of holes, inclusions or cracks. Mathematically, the topological derivative is the first term of the asymptotic expansion of such shape functional with respect to the small parameter which measures the size of the introduced perturbation. In order to clarify the concept of topological derivative, we present below its mathematical definition which can be found in the book by Novotny & Sokołowski [34].

In general, an open and bounded domain $\Omega \subset \mathbb{R}^d$, $d \geq 2$, is perturbed by introducing nonsmooth features confined in a small region $\omega_\varepsilon(\xi)$ of size $\varepsilon > 0$ centred at $\xi \in \Omega$ such that $\overline{\omega_\varepsilon(\xi)} \subset \Omega$. We define a characteristic function having support in the unperturbed domain Ω of the form $\chi = \mathbb{1}_\Omega$. Similarly, we introduce a characteristic function $\chi_\varepsilon(\xi)$

associated to the topologically perturbed domain. For example, in the case of holes as the perturbation $\omega_\varepsilon(\xi)$, we can write $\chi_\varepsilon(\xi) = \mathbb{1}_\Omega - \mathbb{1}_{\overline{\omega_\varepsilon(\xi)}}$ and the singularly perturbed domain can be represented by $\Omega_\varepsilon(\xi) = \Omega \setminus \overline{\omega_\varepsilon(\xi)}$. Further, one assumes that a given shape functional $\psi(\chi_\varepsilon(\xi))$ associated to the topologically perturbed domain $\Omega_\varepsilon(\xi)$ admits the following topological asymptotic expansion

$$\psi(\chi_\varepsilon(\xi)) = \psi(\chi) + f(\varepsilon) D_T\psi(\xi) + o(f(\varepsilon)), \tag{2.1}$$

where $\psi(\chi)$ is the shape functional associated to the reference (unperturbed) domain Ω and $f(\varepsilon)$ is a positive function depending upon the size ε of the topological perturbation such that $f(\varepsilon) \to 0$ when $\varepsilon \downarrow 0$. The function $\xi \mapsto D_T\psi(\xi)$ is called the first order topological derivative of the shape functional ψ at ξ. Mathematically, we can express it as

$$D_T\psi(\xi) := \lim_{\varepsilon\to 0} \frac{\psi(\chi_\varepsilon(\xi)) - \psi(\chi)}{f(\varepsilon)}. \tag{2.2}$$

Similarly, the second order topological derivative of the shape functional ψ at ξ can be obtained by expanding the remainder term $o(f(\varepsilon))$ in (2.1). More precisely, we will get the topological asymptotic expansion

$$\psi(\chi_\varepsilon(\xi)) = \psi(\chi) + f(\varepsilon) D_T\psi(\xi) + f_2(\varepsilon) D_T^2\psi(\xi) + o(f_2(\varepsilon)), \tag{2.3}$$

where $f_2(\varepsilon)$ is such that

$$\lim_{\varepsilon\to 0} \frac{f_2(\varepsilon)}{f(\varepsilon)} = 0. \tag{2.4}$$

Thus, the second order topological derivative can be defined as

$$D_T^2\psi(\xi) := \lim_{\varepsilon\to 0} \frac{\psi(\chi_\varepsilon(\xi)) - \psi(\chi) - f(\varepsilon) D_T\psi(\xi)}{f_2(\varepsilon)}. \tag{2.5}$$

Furthermore, one can define higher order topological derivatives by arguing analogously.

2.2. **Series expansions for Bessel functions.** In this section, we introduce the asymptotic expansion of some modified Bessel functions to be used next.

We denote the modified Bessel functions of the first kind and order n by I_n with $n \in \mathbb{Z}$. As $x \to 0^+$, we have the following asymptotic expansions:

$$I_0(x) = 1 + \frac{1}{4}x^2 + \tilde{I}_0(x), \qquad \tilde{I}_0(x) = O(x^4) \tag{2.6}$$

and

$$I_1(x) = \frac{1}{2}x + \frac{1}{16}x^3 + \tilde{I}_1(x), \qquad \tilde{I}_1(x) = O(x^5). \tag{2.7}$$

The modified Bessel functions of the second kind and order n are denoted by K_n with $n \in \mathbb{Z}$. As $x \to 0^+$, we have the following asymptotic expansions:

$$K_0(x) = (\ln 2 - \zeta) - \ln x - \frac{1}{4}x^2 \ln x + \frac{1}{4}(1 + \ln 2 - \zeta)x^2 + \tilde{K}_0(x), \qquad \tilde{K}_0(x) = O(x^4) \tag{2.8}$$

and

$$K_1(x) = \frac{1}{x} + \frac{1}{2}x\ln x + \frac{1}{2}\left(\zeta - \ln 2 - \frac{1}{2}\right)x + \frac{1}{16}x^3 \ln x + \frac{1}{16}\left(\zeta - \ln 2 - \frac{5}{4}\right)x^3 + \tilde{K}_1(x), \tag{2.9}$$

$\tilde{K}_1(x) = O(x^5)$. In (2.8) and (2.9), ζ is the Euler constant. The above series expansions were obtained from [29, s. 17.7, pp. 276-277].

3. Topology optimization setting

The inverse problem (1.1) has been written in the form of a topology optimization problem (1.5). It is well known that a quite general approach for dealing with such class of problems is based on the concept of topological derivative, which consists in expanding the shape functional $\mathcal{J}_\omega\left(u^1, \cdots, u^M\right)$ with respect to the parameters depend upon a set of small inclusions. Since the topological derivative does not depend on the initial guess of the unknown topology ω^*, we start with the unperturbed domain by setting $\omega = \emptyset$, see Figure 1(b). More precisely, we consider

$$\mathcal{J}_0(u_0^1, \cdots, u_0^M) = \sum_{m=1}^{M} \int_{\Gamma_\circ} (u_0^m - z^m)^2\,, \tag{3.1}$$

where u_0^m be the solution of the unperturbed boundary value problem

$$\left\{ \begin{array}{rcll} -\Delta u_0^m + k u_0^m &=& 0 & \text{in} \quad \Omega, \\ \partial_n u_0^m &=& g_N^m & \text{on} \quad \partial\Omega, \end{array} \right. \tag{3.2}$$

In this paper, we are considering the topology optimization problem (1.5) for the ball-shaped anomalies and hence we define the topologically perturbed counter-part of (3.2) by introducing $N \in \mathbb{Z}^+$ number of small circular inclusions $B_{\varepsilon_i}(x_i)$ with center at $x_i \in \Omega$ and radius ε_i for $i = 1, \cdots, N$. The set of inclusions can be denoted as

$$B_\varepsilon(\xi) = \bigcup_{i=1}^{N} B_{\varepsilon_i}(x_i)\,, \tag{3.3}$$

where $\xi = (x_1, \ldots, x_N)$ and $\varepsilon = (\varepsilon_1, \ldots, \varepsilon_N)$. Moreover, we assume that $\overline{B_\varepsilon} \cap \partial\Omega = \emptyset$ and $\overline{B_{\varepsilon_i}(x_i)} \cap \overline{B_{\varepsilon_j}(x_j)} = \emptyset$ for each $i \neq j$ and $i, j \in \{1, \cdots, N\}$. The shape functional associated with the topologically perturbed domain is written as

$$\mathcal{J}_\varepsilon(u_\varepsilon^1, \cdots, u_\varepsilon^M) = \sum_{m=1}^{M} \int_{\Gamma_\circ} (u_\varepsilon^m - z^m)^2 \tag{3.4}$$

with u_ε^m be the solution of the perturbed boundary value problem

$$\left\{ \begin{array}{rcll} -\Delta u_\varepsilon^m + k_\varepsilon u_\varepsilon^m &=& 0 & \text{in} \quad \Omega, \\ \partial_n u_\varepsilon^m &=& g_N^m & \text{on} \quad \partial\Omega, \end{array} \right. \tag{3.5}$$

where the parameter k_ε is defined as

$$k_\varepsilon = \left\{ \begin{array}{ll} k & \text{in } \Omega \setminus \cup_{i=1}^{N} \overline{B_{\varepsilon_i}(x_i)}, \\ \gamma_i k & \text{in } B_{\varepsilon_i}(x_i)\,. \end{array} \right. \tag{3.6}$$

In order to obtain the topological derivatives of the shape functional $\mathcal{J}_\varepsilon$ at u_ε, we start by simplifying the difference between the perturbed shape functional $\mathcal{J}_\varepsilon\left(u_\varepsilon^1, \cdots, u_\varepsilon^M\right)$ and its unperturbed counter-part $\mathcal{J}_0\left(u_0^1, \cdots, u_0^M\right)$ defined in (3.4) and (3.1), respectively, as follows

$$\mathcal{J}_\varepsilon\left(u_\varepsilon\right) - \mathcal{J}_0\left(u_0\right) = \sum_{m=1}^{M} \int_{\Gamma_\circ} \left[2\left(u_\varepsilon^m - u_0^m\right)\left(u_0^m - z^m\right) + \left(u_\varepsilon^m - u_0^m\right)^2\right], \tag{3.7}$$

where $u_\varepsilon = \left(u_\varepsilon^1, \cdots, u_\varepsilon^M\right)$ and $u_0 = \left(u_0^1, \cdots, u_0^M\right)$.

For $m = 1, \cdots, M$, let us consider the following *ansätz*

$$\begin{aligned} u_\varepsilon^m(x) &= u_0^m(x) + k\sum_{i=1}^{N} |B_{\varepsilon_i}(x_i)|(\gamma_i - 1)h_i^{\varepsilon,m}(x) \\ &\quad + k^2 \sum_{i=1}^{N}\sum_{j=1}^{N} |B_{\varepsilon_i}(x_i)||B_{\varepsilon_j}(x_j)|(\gamma_i - 1)(\gamma_j - 1)h_{ij}^{\varepsilon,m}(x) + \tilde{u}_\varepsilon^m(x), \end{aligned} \tag{3.8}$$

where $|B_{\varepsilon_i}(x_i)|$ is the Lebesgue measure (volume) of the two-dimensional ball $B_{\varepsilon_i}(x_i)$, i.e., $|B_{\varepsilon_i}(x_i)| = \pi\varepsilon_i^2$. Furthermore, for each $i, j = 1, \cdots, N$ and $m = 1, \cdots, M$, $h_i^{\varepsilon,m}$, $h_{ij}^{\varepsilon,m}$ and $\tilde{u}_\varepsilon^m$ are the solutions of

$$\left\{ \begin{array}{rcll} -\Delta h_i^{\varepsilon,m} + k h_i^{\varepsilon,m} &=& -\dfrac{u_0^m}{|B_{\varepsilon_i}(x_i)|}\chi_{B_{\varepsilon_i}(x_i)} & \text{in} \quad \Omega, \\ \partial_n h_i^{\varepsilon,m} &=& 0 & \text{on} \quad \partial\Omega, \end{array} \right. \tag{3.9}$$

$$\left\{ \begin{array}{rcll} -\Delta h_{ij}^{\varepsilon,m} + k h_{ij}^{\varepsilon,m} &=& -\dfrac{h_j^{\varepsilon,m}}{|B_{\varepsilon_i}(x_i)|}\chi_{B_{\varepsilon_i}(x_i)} & \text{in} \quad \Omega, \\ \partial_n h_{ij}^{\varepsilon,m} &=& 0 & \text{on} \quad \partial\Omega, \end{array} \right. \tag{3.10}$$

and

$$\left\{ \begin{array}{rcll} -\Delta \tilde{u}_\varepsilon^m + k_\varepsilon \tilde{u}_\varepsilon^m &=& \Phi_\varepsilon^m & \text{in } \Omega, \\ \partial_n \tilde{u}_\varepsilon^m &=& 0 & \text{on } \partial\Omega, \end{array} \right. \tag{3.11}$$

respectively. In problem (3.11), we have

$$\Phi_\varepsilon^m = -k^3 \sum_{i=1}^{N}\sum_{j=1}^{N}\sum_{l=1}^{N} |B_{\varepsilon_j}(x_j)||B_{\varepsilon_l}(x_l)|(\gamma_i - 1)(\gamma_j - 1)(\gamma_l - 1)h_{jl}^{\varepsilon,m}\chi_{B_{\varepsilon_i}(x_i)}. \tag{3.12}$$

To simplify the notation, let us introduce the quantities

$$\alpha_i = |B_{\varepsilon_i}(x_i)| \quad \text{and} \quad \beta_i = (\gamma_i - 1), \tag{3.13}$$

for $i = 1, \cdots, N$, from which we define the vector

$$\alpha = (\alpha_1, \cdots, \alpha_N). \tag{3.14}$$

By using (3.13), the expansion (3.8) will have the form

$$u_\varepsilon^m(x) = u_0^m(x) + k\sum_{i=1}^{N} \alpha_i\beta_i h_i^{\varepsilon,m}(x) + k^2\sum_{i=1}^{N}\sum_{j=1}^{N} \alpha_i\alpha_j\beta_i\beta_j h_{ij}^{\varepsilon,m}(x) + \tilde{u}_\varepsilon^m(x). \tag{3.15}$$

In order to simplify further analysis, we write $h_i^{\varepsilon,m}$ as a sum of three functions p_i^ε, q_i and $\tilde{h}_i^{\varepsilon,m}$ in the form

$$h_i^{\varepsilon,m} = u_0^m(x_i)h_i^\varepsilon + \tilde{h}_i^{\varepsilon,m} \quad \text{with} \quad h_i^\varepsilon = p_i^\varepsilon + q_i^\varepsilon. \tag{3.16}$$

The function p_i^ε is solution of

$$\left\{\begin{array}{rcll} -\Delta p_i^\varepsilon + k p_i^\varepsilon & = & -\dfrac{1}{|B_{\varepsilon_i}(x_i)|}\chi_{B_{\varepsilon_i}(x_i)} & \text{in } B_R(x_i), \\ p_i^\varepsilon & = & \lambda_3^{\varepsilon_i} K_0(\sqrt{k}R) & \text{on } \partial B_R(x_i), \end{array}\right. \tag{3.17}$$

with $B_{\varepsilon_i}(x_i) \subset \Omega \subset B_R(x_i)$, $x_i \in \Omega$, $0 < \varepsilon_i \ll R$. Moreover, $\lambda_3^{\varepsilon_i}$ denotes a constant depending on ε_i to be presented next. Problem (3.17) can be solved analytically and its solution is

$$p_i^\varepsilon(x) = \left\{\begin{array}{ll} \lambda_1^{\varepsilon_i} + \lambda_2^{\varepsilon_i} I_0(\sqrt{k}\|x - x_i\|) & \text{in } B_{\varepsilon_i}(x_i), \\ \lambda_3^{\varepsilon_i} K_0(\sqrt{k}\|x - x_i\|) & \text{in } B_R(x_i) \setminus \overline{B_{\varepsilon_i}(x_i)}, \end{array}\right. \tag{3.18}$$

with

$$\lambda_1^{\varepsilon_i} = -\frac{1}{k\pi\varepsilon_i^2}, \tag{3.19}$$

$$\lambda_2^{\varepsilon_i} = \frac{1}{k\pi\varepsilon_i^2} \frac{K_1(\sqrt{k}\varepsilon_i)}{K_0(\sqrt{k}\varepsilon_i) I_1(\sqrt{k}\varepsilon_i) + K_1(\sqrt{k}\varepsilon_i) I_0(\sqrt{k}\varepsilon_i)}, \tag{3.20}$$

and

$$\lambda_3^{\varepsilon_i} = -\frac{1}{k\pi\varepsilon_i^2} \frac{I_1(\sqrt{k}\varepsilon_i)}{K_0(\sqrt{k}\varepsilon_i) I_1(\sqrt{k}\varepsilon_i) + K_1(\sqrt{k}\varepsilon_i) I_0(\sqrt{k}\varepsilon_i)}. \tag{3.21}$$

We can use the asymptotic expansions (2.6)-(2.9) to rewrite (3.20) and (3.21) as follows

$$\lambda_2^{\varepsilon_i} = \frac{1}{k\pi\varepsilon_i^2} + \lambda + \frac{1}{2\pi}\ln\varepsilon_i + \tilde{\lambda}_2^{\varepsilon_i}, \qquad \tilde{\lambda}_2^{\varepsilon_i} = O(\varepsilon_i^2), \tag{3.22}$$

with

$$\lambda = \frac{1}{4\pi}(2\zeta + \ln k - 2\ln 2 - 1) \tag{3.23}$$

and

$$\lambda_3^{\varepsilon_i} = -\frac{1}{2\pi} + \tilde{\lambda}_3^{\varepsilon_i}, \qquad \tilde{\lambda}_3^{\varepsilon_i} = O(\varepsilon_i^2). \tag{3.24}$$

Taking into account the solution p_i^ε of the problem (3.17), we write $q_i^\varepsilon = \lambda_3^{\varepsilon_i} q_i$, where q_i is the solution to the homogeneous boundary value problem

$$\left\{\begin{array}{rcll} -\Delta q_i + k q_i & = & 0 & \text{in } \Omega, \\ \partial_n q_i & = & -\partial_n K_0(\sqrt{k}\|x - x_i\|) & \text{on } \partial\Omega \end{array}\right. \tag{3.25}$$

and $\tilde{h}_i^{\varepsilon,m}$ solves the boundary value problem

$$\left\{\begin{array}{rcll} -\Delta \tilde{h}_i^{\varepsilon,m} + k\tilde{h}_i^{\varepsilon,m} & = & -\dfrac{1}{|B_{\varepsilon_i}(x_i)|}\left(u_0^m - u_0^m(x_i)\right)\chi_{B_{\varepsilon_i}(x_i)} & \text{in } \Omega, \\ \partial_n \tilde{h}_i^{\varepsilon,m} & = & 0 & \text{on } \partial\Omega. \end{array}\right. \tag{3.26}$$

From the decomposition (3.16) and the solution of the problem (3.17), we can introduce the notation

$$h_i^{\varepsilon,m} := \left\{\begin{array}{ll} u_0^m(x_i) h^\varepsilon_{i|_{B_{\varepsilon_i}}} + \tilde{h}_i^{\varepsilon,m} & \text{in } B_{\varepsilon_i}(x_i), \\ u_0^m(x_i) h^\varepsilon_{i|_{\Omega\setminus\overline{B_{\varepsilon_i}}}} + \tilde{h}_i^{\varepsilon,m} & \text{in } \Omega \setminus \overline{B_{\varepsilon_i}(x_i)}, \end{array}\right. \tag{3.27}$$

with

$$h^\varepsilon_{i|_{B_{\varepsilon_i}}} := p^\varepsilon_{i|_{B_{\varepsilon_i}}} + \lambda_3^{\varepsilon_i} q_i \quad \text{and} \quad h^\varepsilon_{i|_{\Omega\setminus\overline{B_{\varepsilon_i}}}} := p^\varepsilon_{i|_{\Omega\setminus\overline{B_{\varepsilon_i}}}} + \lambda_3^{\varepsilon_i} q_i, \tag{3.28}$$

where $p^\varepsilon_{i|_{B_{\varepsilon_i}}}$ is the solution of the problem (3.17) in $B_{\varepsilon_i}(x_i)$ and $p^\varepsilon_{i|_{\Omega\setminus\overline{B_{\varepsilon_i}}}}$ is the solution of the same problem in $\Omega \setminus \overline{B_{\varepsilon_i}(x_i)}$. Moreover, we also introduce an adjoint state v^m as the solution of the following auxiliary boundary value problem

$$\begin{cases} -\Delta v^m + kv^m &= 0 & \text{in } \Omega, \\ \partial_n v^m &= 0 & \text{on } \partial\Omega \setminus \Gamma_\circ, \\ \partial_n v^m &= u_0^m - z^m & \text{on } \Gamma_\circ. \end{cases} \tag{3.29}$$

4. Main theorem

In this section, we state our main result which consists in the closed form of the topological derivatives appear in the topological asymptotic expansion of the perturbed cost functional. Let us first introduce the vector $d \in \mathbb{R}^N$ and the matrices $G,\ H \in \mathbb{R}^{N\times N}$ whose entries are defined as

$$d_i := 2k\beta_i \sum_{m=1}^{M} u_0^m(x_i)v^m(x_i), \tag{4.1}$$

$$G_{ii} := -\frac{1}{2\pi}k^2\beta_i^2 \sum_{m=1}^{M} u_0^m(x_i)v^m(x_i), \quad G_{ij} = 0, \quad \text{if} \quad i \neq j \tag{4.2}$$

and

$$\begin{aligned} H_{ii} \ := \ & -\frac{1}{\pi}k^2\beta_i \sum_{m=1}^{M} u_0^m(x_i)v^m(x_i) - \frac{1}{\pi}k\beta_i \sum_{m=1}^{M} \nabla u_0^m(x_i)\cdot\nabla v^m(x_i) \\ & -\frac{1}{2\pi}\sigma k^2\beta_i^2 \sum_{m=1}^{M} u_0^m(x_i)v^m(x_i) + \frac{2}{\pi}k^2\beta_i^2 \sum_{m=1}^{M} u_0^m(x_i)v^m(x_i)q_i(x_i) \\ & +\frac{1}{2\pi^2}k^2\beta_i^2 \sum_{m=1}^{M} [u_0^m(x_i)]^2\, \mathcal{I}_{ii}, \end{aligned} \tag{4.3}$$

$$\begin{aligned} H_{ij} \ := \ & \frac{2}{\pi}k^2\beta_i\beta_j \sum_{m=1}^{M} u_0^m(x_j)v^m(x_i)\mathcal{K}_{ij} + \frac{2}{\pi}k^2\beta_i\beta_j \sum_{m=1}^{M} u_0^m(x_j)v^m(x_i)q_j(x_i) \\ & +\frac{1}{2\pi^2}k^2\beta_i\beta_j \sum_{m=1}^{M} u_0^m(x_i)u_0^m(x_j)\, \mathcal{I}_{ij}, \end{aligned} \tag{4.4}$$

if $i \neq j$; respectively, for $i, j = 1, \cdots, N$. In (4.3), σ is a constant given by

$$\sigma = -1 + 4\zeta + \ln\frac{k^2}{16\pi^2} \tag{4.5}$$

with ζ denoting the Euler constant. Moreover, for $i, j = 1, \cdots, N$, $\mathcal{K}_{ij}$ and $\mathcal{I}_{ij}$ appearing in (4.3)-(4.4) are, respectively, a number given by

$$\mathcal{K}_{ij} = K_0(\sqrt{k}\|x_i - x_j\|), \tag{4.6}$$

and an integral defined as

$$\mathcal{I}_{ij} = \int_{\Gamma_\circ} [K_0(\sqrt{k}\|x - x_i\|) + q_i\,(x)][K_0(\sqrt{k}\|x - x_j\|) + q_j\,(x)], \tag{4.7}$$

where $K_0(x)$ denotes the modified Bessel function of the second kind and zero order. We are now in position to state the main result of this paper.

Theorem 1. *Let q_i for $i = 1, \cdots, N$ and u_0^m, v^m for $m = 1, \cdots, M$ be the functions defined in* (3.25) *and* (3.2), (3.29), *respectively. Additionally, let d, G and H be the vector and the matrices whose entries are defined in* (4.1), (4.2) *and* (4.3)-(4.4), *respectively. Then, for the vector α introduced in* (3.13), *we have the following asymptotic expansion for the topologically perturbed cost functional $\psi(\chi_\varepsilon(\xi)) := \mathcal{J}_\varepsilon(u_\varepsilon)$ defined in* (3.4)*:*

$$\psi(\chi_\varepsilon(\xi)) = \psi(\chi) - \alpha \cdot d(\xi) + G(\xi)\alpha \cdot \mathrm{diag}(\alpha \otimes \ln \alpha) + \frac{1}{2} H(\xi)\alpha \cdot \alpha + o(|\alpha|^2), \tag{4.8}$$

where $\psi(\chi) := \mathcal{J}_0(u_0)$ is the topologically unperturbed cost functional from (3.1).

Proof. The reader interested in the proof of this result may refer to Appendix A. □

5. A noniterative reconstruction algorithm

The optimization problem (1.5) to find the approximation $\omega^\star$ to ω^* is solved by using a noniterative scheme devised from the topological asymptotic expansion of the shape functional $\mathcal{J}_\varepsilon(u_\varepsilon)$ given by (4.8). We start by disregarding the terms of order $o(|\alpha|^2)$ in (4.8), which leads us to the truncated expansion written as

$$\delta J(\alpha, \xi, N) := -\alpha \cdot d(\xi) + G(\xi)\alpha \cdot \mathrm{diag}(\alpha \otimes \ln \alpha) + \frac{1}{2} H(\xi)\alpha \cdot \alpha. \tag{5.1}$$

Since we are looking for the pair $(\alpha^\star, \xi^\star)$ which minimizes (5.1) for a given number N of anomalies, we differentiate $\delta J(\alpha, \xi, N)$ with respect to the variable α to obtain the first order optimality condition given by the following non-linear system

$$(H(\xi) + G(\xi))\,\alpha + 2G(\xi)\mathrm{diag}(\alpha \otimes \log \alpha) = d(\xi), \tag{5.2}$$

where the entries of the vector $d \in \mathbb{R}^N$ and the matrices $G, H \in \mathbb{R}^N \times \mathbb{R}^N$ are given by (4.1), (4.2) and (4.3)-(4.4), respectively. The non-linear system (5.2) is solved by using Newton's method. Note that, if α is solution of the system (5.2), then it becomes a function of the locations ξ, that is, $\alpha = \alpha(\xi)$. Let us now replace the solution of (5.2) into $\delta J(\alpha, \xi, N)$ to obtain

$$\delta J(\alpha(\xi), \xi, N) = -\frac{1}{2}(d(\xi) + G(\xi)\alpha(\xi)) \cdot \alpha(\xi). \tag{5.3}$$

Therefore, the pair of vectors $(\xi^\star, \alpha^\star)$ which minimizes (5.1) is given by

$$\xi^\star := \underset{\xi \in X}{\mathrm{argmin}}\ \delta J(\alpha(\xi), \xi, N) \quad \text{and} \quad \alpha^\star := \alpha(\xi^\star), \tag{5.4}$$

where X denotes a set of admissible anomalies locations.

In summary, for a given number N of trial inclusions, the reconstruction algorithm is able to find in one step their locations $\xi^\star$ and sizes $\alpha^\star$. We highlight some features of the proposed algorithm. Firstly, it is noniterative and independent of initial guess, which makes it very robust with respect to noisy data. On the other hand, the approximation of any anomaly ω^* by a ball-shaped inclusion $\omega^\star$ can be seen as a limitation of our approach. Despite this, our algorithm can be used to get a good initial guess for iterative approaches such as those based on level-set methods [7, 28], for instance. The algorithm can be found in pseudo-code format in [33].

6. Numerical examples

The algorithm described in the previous section is applied to several examples to demonstrate the effectiveness of our approach. The numerical examples are conducted in scenarios of complete and partial boundary measurements in order to investigate the capability of the proposed method in reconstructing multiple anomalies of different sizes and shapes. We also have tested the robustness of the reconstruction with respect to noisy data.

The reference geometrical domain is given by a square $\Omega = (-0.5, 0.5) \times (-0.5, 0.5)$ which is discretized with three-node finite elements. The mesh is generated from a grid of 160×160 squares. Each square is divided into four triangles which leads to a resulting mesh comprising 102400 elements and 51521 nodes. The boundary of the geometrical domain $\partial\Omega$ is excited by imposing three different Neumann data, namely, $g_N^1 = 1$, $g_N^2 = x$ and $g_N^3 = y$. The associated potential g_D^m, for $m = 1, 2, 3$, is measured on the whole boundary $\Gamma_\circ = \partial\Omega$ or on a part of it $\Gamma_\circ \subsetneq \partial\Omega$. The material property of the background is assumed to be uniform and given by $k = 1$. For a number M of measurements, the objective is to reconstruct a number N^* of anomalies with contrast $\gamma_i = \gamma$, $\gamma \in \mathbb{R}^+$, for $i = 1, \cdots, N^*$, from the help of measurements of the potential g_D^m taken in $\Gamma_\circ$.

For a fixed unknown number of inclusions N which we are going to find, the solution α of the non-linear system (5.2) requires the entries of the vector $d \in \mathbb{R}^N$ and the matrices $G, H \in \mathbb{R}^N \times \mathbb{R}^N$ which, in turn, are dependent on the computation of the functions u_0^m, q_i and v^m - see equations (4.1)-(4.4). These functions, solutions of the auxiliary boundary value problems (3.2), (3.25) and (3.29), respectively, are computed over the mentioned resulting mesh. The combinatorial search is performed on a sub-grid X consisting of uniformly distributed points extracted from the mesh. For all examples below, we consider a fixed sub-grid X comprising 181 points such that the optimal solution $(\xi^\star, \alpha^\star)$ is defined in X.

In the case of noisy data, the parameter k_{ω^*} is replaced by $k_{\omega^*}^{\mu} = k_{\omega^*}(1 + \mu\tau)$, where τ is a random variable taking values in the interval $(-1, 1)$ and μ corresponds to the noise level.

6.1. Complete boundary measurements.

In this section, we present three examples concerning total boundary measurements, i.e., for a boundary excitation (through the Neumann data g_N^m, $m = \{1, 2, 3\}$) imposed on $\partial\Omega$, the corresponding boundary measurement (through the associated potential g_D^m) is taken on the whole boundary $\Gamma_\circ = \partial\Omega$. The first example analyses the sensitivity of the reconstruction with respect to the contrast. In the second one, two anomalies of different shapes and sizes are approximated by a number of trial balls. Finally, in the third example, we investigate the robustness of the reconstruction method with respect to the noisy data.

6.1.1. *Example 1.*

Sensitivity of the reconstruction with respect to the contrast $\gamma \in \mathbb{R}^+$ is analysed in this example. In this case, we consider a single anomaly to be reconstructed from one boundary measurement. The target anomaly ω^* is given by a circular region with radius $\varepsilon^* = 0.05$ and center located at the origin i.e., $x^* = (0, 0)$. The boundary of the domain is excited by imposing the Neumann data $g_N^1 = 1$. The values for the contrast γ were taken in the form $\gamma = 2^s$ with $s \in [-7, 7] \subset \mathbb{Z} \setminus \{0\}$. The center x^* of the anomaly ω^* was successfully found for all values of γ. Concerning to the size ε^* of the anomaly, one can state that the higher is the value of the contrast, the more underestimated is the predicted radius $\varepsilon^\star$. See Figure 2 where we have plotted the obtained radius $\varepsilon^\star$ on vertical axis against the value of γ on horizontal axis. From now on, for any number N^* of anomalies we are going to reconstruct, we take the value of the contrast as $\gamma_i = 2$, for $i = 1, \cdots, N^*$.

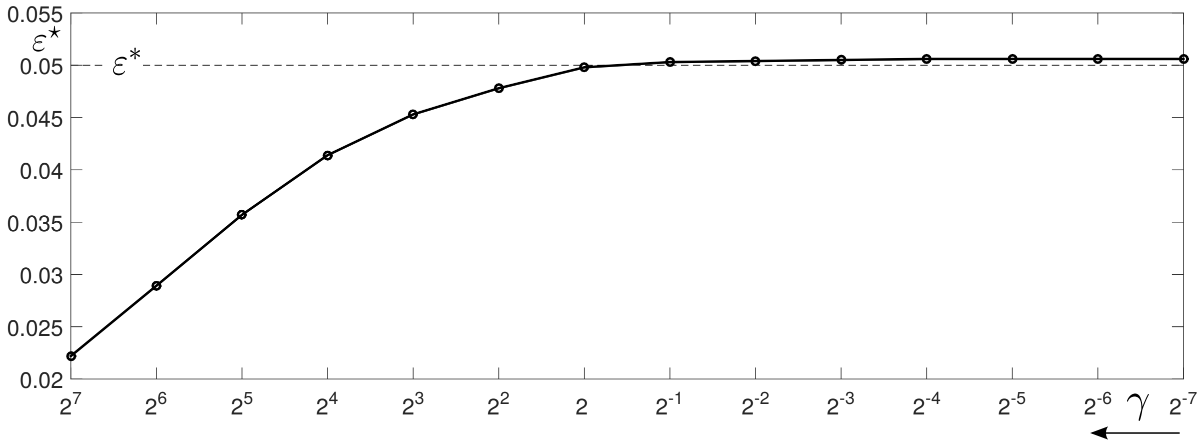

FIGURE 2. Example 1: The approximated solution $\varepsilon^\star$ for different values of γ.

6.1.2. *Example 2.* In this example, we detect the topology as well as the shape of the anomalies. The target domain contains two anomalies such that one of them is a square-shaped anomaly while the other is a small circular region, as shown in Figure 3(a). The reconstruction of two anomalies of different shapes induces us to increase the number of measurements due to the need for more information to achieve a satisfactory result. In fact, Figure 3(b) shows us the reconstruction when only one measurement is considered with the Neumann data $g_N^2 = x$. Such a result can be improved by taking into account all the Neumann data simultaneously, i.e., the reconstruction is performed from the measurements obtained with $g_N^1 = 1$, $g_N^2 = x$ and $g_N^3 = y$. In this case, the square-shaped anomaly is approximated by a ball-shaped geometry which has approximately the same volume and its center coincides with the centroid of the square. Concerning to the circular anomaly, the reconstruction process accurately found its exact center and the radius obtained is approximately equal to the true value. We demonstrate the numerical result in the Figure 3(c). The results obtained here motivate us to take into account all the three boundary excitations g_N^1, g_N^2 and g_N^3 in the forthcoming examples of reconstructing multiple anomalies.

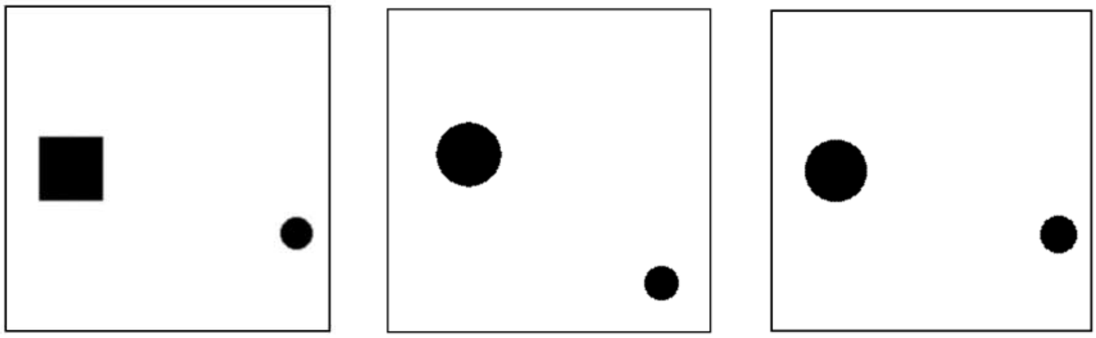

(a) target (b) result with $M = 1$ (c) result with $M = 3$

FIGURE 3. Example 2.

6.1.3. *Example 3.* The robustness of the method with respect to noisy data is investigated in this example. The target consists of three embedded anomalies of same size, as illustrated in Figure 4(a)(left). The anomalies are accurately reconstructed in the absence of noise. This result is demonstrated in Figure 4(a)(right). The parameter k_{ω^*} is now corrupted with different levels of noise. We illustrate the target domains corresponding to the cases where k_{ω^*} is corrupted with level of noise equal to $\mu = 20\%$, $\mu = 40\%$ and $\mu = 50\%$ on the left side of the Figures 4(b), 4(c) and 4(d), respectively. From the results presented on the right side of the Figure 5, we can observe that the anomalies are reconstructed successfully for levels of noise up to 40%. The reconstruction is completely degraded for levels of noise greater than 40%, as can be seen in Figure 4(d)(right).

6.2. **Partial boundary measurements.** We present one last example concerning to partial boundary measurements which means we impose boundary excitations g_N^m $(m = 1, 2, 3)$ on whole $\partial\Omega$ but we collect the boundary measurements of the potential g_D^m just on a part of it $\Gamma_\circ \subsetneq \partial\Omega$. In particular, we consider the boundary $\Gamma_\circ$ as the union of eight disjoint parts which are represented by thick black lines in Figure 5.

6.2.1. *Example 4.* The target consists of two ball-shaped anomalies of different sizes which is corrupted with different levels of noise. We illustrate the target domain in the absence of noise in Figure 5(a)(left). On the left side of the Figures 5(b)-5(d), we present the target domains corresponding to the cases where the parameter k_{ω^*} is corrupted with level of noise $\mu = 20\%$, $\mu = 40\%$ and $\mu = 50\%$, respectively. Anomalies are successfully reconstructed in the absence of noise, as can be seen in 5(a)(right). For levels of noise up to 40% the reconstruction scheme is able to find the exact centers of the anomalies and the obtained radii are approximately equal to the true values. The reconstruction starts to be degraded for levels of noise greater than 40%. These results are demonstrated in Figures 5(b)-5(d). Through this example, we can verify that the proposed method is robustness with respect to noisy data even in scenarios of partial boundary measurements.

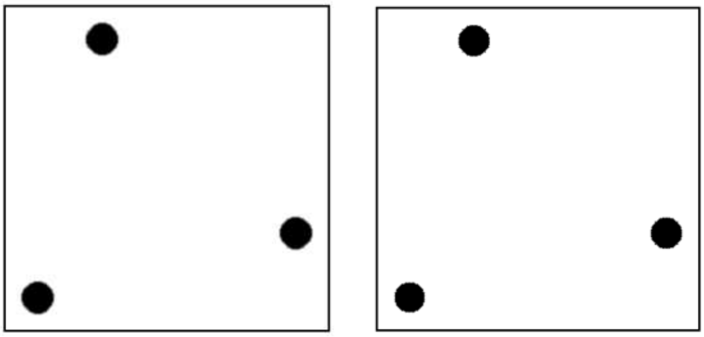

(a) $\mu = 0\%$

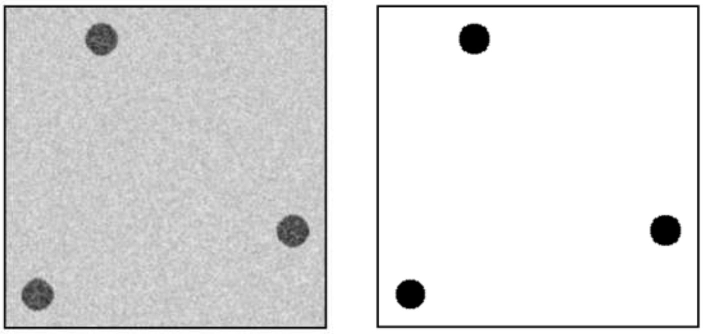

(b) $\mu = 20\%$

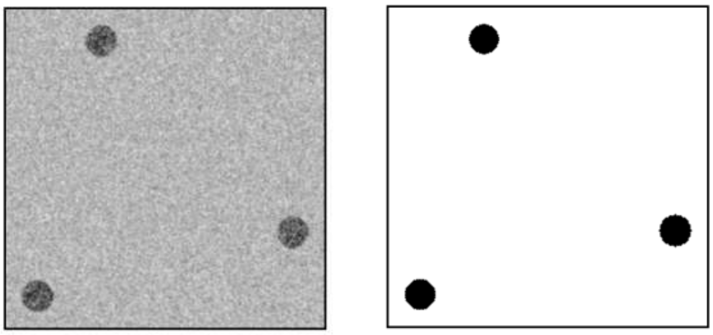

(c) $\mu = 40\%$

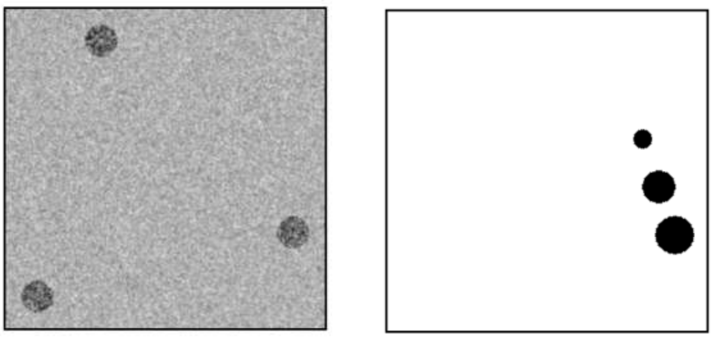

(d) $\mu = 50\%$

FIGURE 4. Example 3: Target (left) and the respective result (right) for different levels of noise.

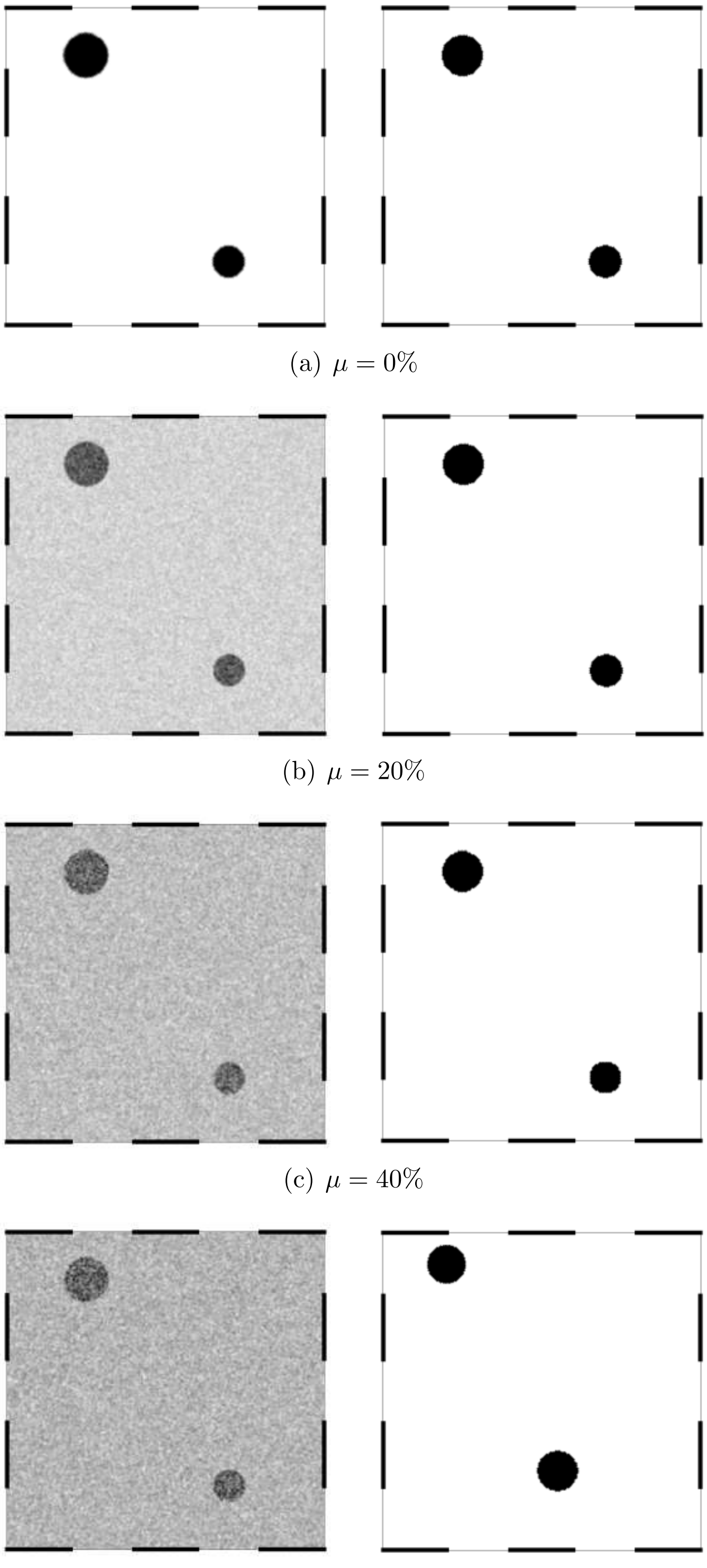

(a) $\mu = 0\%$

(b) $\mu = 20\%$

(c) $\mu = 40\%$

(d) $\mu = 50\%$

FIGURE 5. Example 4: Target (left) and the respective result (right) for different levels of noise.

7. Conclusions

In the paper we have considered the open problem discussed in the book by Isakov [27, pp. 126, Problem 4.2]. In particular, a noniterative reconstruction method for solving the above inverse problem has been proposed. The general idea consists in rewrite the inverse problem as a topology optimization problem, where a shape functional measuring the misfit between the boundary measurements and the solution obtained from the model is expanded with respect to a set of ball-shaped anomalies and then truncated up to the desired order term. The truncated expansion has been used to devise a noniterative reconstruction algorithm based on a simple optimization step, which has been proved to be very robust with respect to noisy data and also independent of any initial guess. On the other hand, approximating the solution to the inverse problem by a finite number of balls can be seen as a limitation of our approach. However, the reconstruction obtained may serve as an initial guess for other well-established and more computationally sophisticated iterative methods [7, 10, 25, 28, 39].

Appendix A. Proof of the main result

The proof of Theorem 1 is demonstrated in three steps. Firstly, we develop the asymptotic expansion of the topologically perturbed cost functional. Next, we prove *a priori* estimates related to the auxiliary states $\tilde{h}_i^{\varepsilon,m}$, $h_i^{\varepsilon,m}$, $h_{ij}^{\varepsilon,m}$ and $\tilde{u}_\varepsilon^m$ for $i,j = 1,\cdots,N$ and $m = 1,\cdots,M$. Finally, in the last part of this section, the previously obtained results are used to estimate the remainders appeared in the first step. These estimates justify our topological asymptotic expansion (A.30).

A.1. **Asymptotic development of the shape functional.** Let us use (3.15) in (3.7), to obtain

$$\begin{aligned}\mathcal{J}_\varepsilon(u_\varepsilon) - \mathcal{J}_0(u_0) = 2k \sum_{m=1}^{M}\sum_{i=1}^{N} \alpha_i\beta_i \int_{\Gamma_\circ} h_i^{\varepsilon,m}(u_0^m - z^m) \\ + 2k^2 \sum_{m=1}^{M}\sum_{i=1}^{N}\sum_{j=1}^{N} \alpha_i\alpha_j\beta_i\beta_j \int_{\Gamma_\circ} h_{ij}^{\varepsilon,m}(u_0^m - z^m) \\ + k^2 \sum_{m=1}^{M}\sum_{i=1}^{N}\sum_{j=1}^{N} \alpha_i\alpha_j\beta_i\beta_j \int_{\Gamma_\circ} h_i^{\varepsilon,m} h_j^{\varepsilon,m} + \sum_{m=1}^{M}\sum_{\ell=1}^{6} \mathcal{E}_\ell^m(\varepsilon), \quad \text{(A.1)}\end{aligned}$$

where

$$\mathcal{E}_1^m(\varepsilon) = 2\int_{\Gamma_\circ} \tilde{u}_\varepsilon^m (u_0^m - z^m), \quad \text{(A.2)}$$

$$\mathcal{E}_2^m(\varepsilon) = 2k^3 \sum_{i=1}^{N}\sum_{j=1}^{N}\sum_{l=1}^{N} \alpha_i\alpha_j\alpha_l\beta_i\beta_j\beta_l \int_{\Gamma_\circ} h_i^{\varepsilon,m} h_{jl}^{\varepsilon,m}, \quad \text{(A.3)}$$

$$\mathcal{E}_3^m(\varepsilon) = 2k \sum_{i=1}^{N} \alpha_i\beta_i \int_{\Gamma_\circ} h_i^{\varepsilon,m} \tilde{u}_\varepsilon^m, \quad \text{(A.4)}$$

$$\mathcal{E}_4^m(\varepsilon) = k^4 \sum_{i=1}^N \sum_{j=1}^N \sum_{l=1}^N \sum_{p=1}^N \alpha_i \alpha_j \alpha_l \alpha_p \beta_i \beta_j \beta_l \beta_p \int_{\Gamma_\circ} h_{ij}^{\varepsilon,m} h_{lp}^{\varepsilon,m}, \tag{A.5}$$

$$\mathcal{E}_5^m(\varepsilon) = 2k^2 \sum_{i=1}^N \sum_{j=1}^N \alpha_i \alpha_j \beta_i \beta_j \int_{\Gamma_\circ} h_{ij}^{\varepsilon,m} \tilde{u}_\varepsilon^m \tag{A.6}$$

and

$$\mathcal{E}_6^m(\varepsilon) = \int_{\Gamma_\circ} (\tilde{u}_\varepsilon^m)^2 . \tag{A.7}$$

Now, let us introduce the weak formulation of the adjoint problem (3.29) which is to find $v^m \in H^1(\Omega)$ such that

$$\int_\Omega \nabla v^m \cdot \nabla \eta + k \int_\Omega v^m \eta = \int_{\Gamma_\circ} (u_0^m - z^m)\, \eta, \quad \forall \eta \in H^1(\Omega). \tag{A.8}$$

The weak formulations of the problems (3.9) and (3.10) are to find $h_i^{\varepsilon,m} \in H^1(\Omega)$ such that

$$\int_\Omega \nabla h_i^{\varepsilon,m} \cdot \nabla \eta + k \int_\Omega h_i^{\varepsilon,m} \eta = -\frac{1}{\alpha_i} \int_{B_{\varepsilon_i}(x_i)} u_0^m \eta, \quad \forall \eta \in H^1(\Omega) \tag{A.9}$$

and $h_{ij}^{\varepsilon,m} \in H^1(\Omega)$ such that

$$\int_\Omega \nabla h_{ij}^{\varepsilon,m} \cdot \nabla \eta + k \int_\Omega h_{ij}^{\varepsilon,m} \eta = -\frac{1}{\alpha_i} \int_{B_{\varepsilon_i}(x_i)} h_j^{\varepsilon,m} \eta, \quad \forall \eta \in H^1(\Omega), \tag{A.10}$$

respectively. By taking $\eta = h_i^{\varepsilon,m}$ in (A.8) and $\eta = v^m$ in (A.9) as test functions, we get

$$\int_{\Gamma_\circ} h_i^{\varepsilon,m} (u_0^m - z^m) = -\frac{1}{\alpha_i} \int_{B_{\varepsilon_i}(x_i)} u_0^m v^m. \tag{A.11}$$

Similarly, if we take $\eta = h_{ij}^{\varepsilon,m}$ in (A.8) and $\eta = v^m$ in (A.10) as test functions, it gives

$$\int_{\Gamma_\circ} h_{ij}^{\varepsilon,m} (u_0^m - z^m) = -\frac{1}{\alpha_i} \int_{B_{\varepsilon_i}(x_i)} h_j^{\varepsilon,m} v^m. \tag{A.12}$$

By using (A.11) and (A.12) in (A.1), we get

$$\begin{aligned} \mathcal{J}_\varepsilon(u_\varepsilon) - \mathcal{J}_0(u_0) = & -2k \sum_{m=1}^M \sum_{i=1}^N \beta_i \int_{B_{\varepsilon_i}(x_i)} u_0^m v^m - 2k^2 \sum_{m=1}^M \sum_{i=1}^N \sum_{j=1}^N \alpha_j \beta_i \beta_j \int_{B_{\varepsilon_i}(x_i)} h_j^{\varepsilon,m} v^m \\ & + k^2 \sum_{m=1}^M \sum_{i=1}^N \sum_{j=1}^N \alpha_i \alpha_j \beta_i \beta_j \int_{\Gamma_\circ} h_i^{\varepsilon,m} h_j^{\varepsilon,m} + \sum_{m=1}^M \sum_{\ell=1}^6 \mathcal{E}_\ell^m(\varepsilon) . \end{aligned} \tag{A.13}$$

Taking into account the decomposition (3.27), we get

$$\mathcal{J}_\varepsilon(u_\varepsilon) - \mathcal{J}_0(u_0) = -2k\sum_{m=1}^{M}\sum_{i=1}^{N}\beta_i\int_{B_{\varepsilon_i}(x_i)} u_0^m v^m$$

$$-2k^2\sum_{m=1}^{M}\sum_{i=1}^{N}\alpha_i\beta_i^2 u_0^m(x_i)\int_{B_{\varepsilon_i}(x_i)} h^\varepsilon_{i\,|_{B_{\varepsilon_i}}} v^m - 2k^2\sum_{m=1}^{M}\sum_{i=1}^{N}\sum_{\substack{j=1\\ j\neq i}}^{N}\alpha_j\beta_i\beta_j u_0^m(x_j)\int_{B_{\varepsilon_i}(x_i)} h^\varepsilon_{j\,|_{\Omega\setminus\overline{B_{\varepsilon_j}}}} v^m$$

$$+k^2\sum_{m=1}^{M}\sum_{i=1}^{N}\sum_{j=1}^{N}\alpha_i\alpha_j\beta_i\beta_j u_0^m(x_i)\,u_0^m(x_j)\int_{\Gamma_\circ} h^\varepsilon_{i\,|_{\Omega\setminus\overline{B_{\varepsilon_i}}}} h^\varepsilon_{j\,|_{\Omega\setminus\overline{B_{\varepsilon_j}}}} + \sum_{m=1}^{M}\sum_{\ell=1}^{10}\mathcal{E}_\ell^m(\varepsilon). \quad \text{(A.14)}$$

Here, the four new remainders are defined as

$$\mathcal{E}_7^m(\varepsilon) = k^2\sum_{i=1}^{N}\sum_{j=1}^{N}\alpha_i\alpha_j\beta_i\beta_j\int_{\Gamma_\circ}\left(u_0^m(x_i)\,h^\varepsilon_{i\,|_{\Omega\setminus\overline{B_{\varepsilon_i}}}}\tilde{h}_j^{\varepsilon,m} + u_0^m(x_j)\,h^\varepsilon_{j\,|_{\Omega\setminus\overline{B_{\varepsilon_j}}}}\tilde{h}_i^{\varepsilon,m}\right), \quad \text{(A.15)}$$

$$\mathcal{E}_8^m(\varepsilon) = k^2\sum_{i=1}^{N}\sum_{j=1}^{N}\alpha_i\alpha_j\beta_i\beta_j\int_{\Gamma_\circ}\tilde{h}_i^{\varepsilon,m}\tilde{h}_j^{\varepsilon,m}, \quad \text{(A.16)}$$

$$\mathcal{E}_9^m(\varepsilon) = -2k^2\sum_{i=1}^{N}\alpha_i\beta_i^2\int_{B_{\varepsilon_i}(x_i)}\tilde{h}_i^{\varepsilon,m}v^m, \quad \text{(A.17)}$$

$$\mathcal{E}_{10}^m(\varepsilon) = -2k^2\sum_{i=1}^{N}\sum_{\substack{j=1\\ j\neq i}}^{N}\alpha_j\beta_i\beta_j\int_{B_{\varepsilon_i}(x_i)}\tilde{h}_j^{\varepsilon,m}v^m. \quad \text{(A.18)}$$

By using the notations introduced in (3.28) and the analytical form of p_i^ε given by (3.18), the asymptotic expansion (A.14) takes the form

$$\mathcal{J}_\varepsilon(u_\varepsilon) - \mathcal{J}_0(u_0) = -2k\sum_{m=1}^{M}\sum_{i=1}^{N}\beta_i\int_{B_{\varepsilon_i}(x_i)} u_0^m v^m - 2k^2\sum_{m=1}^{M}\sum_{i=1}^{N}\alpha_i^2\lambda_1^{\varepsilon_i}\beta_i^2 u_0^m(x_i)\,v^m(x_i)$$

$$-2k^2\sum_{m=1}^{M}\sum_{i=1}^{N}\alpha_i\lambda_2^{\varepsilon_i}\mathcal{I}^{\varepsilon_i}\beta_i^2 u_0^m(x_i)\,v^m(x_i) - 2k^2\sum_{m=1}^{M}\sum_{i=1}^{N}\alpha_i^2\lambda_3^{\varepsilon_i}\beta_i^2 u_0^m(x_i)\,v^m(x_i)\,q_i(x_i)$$

$$-2k^2\sum_{m=1}^{M}\sum_{i=1}^{N}\sum_{\substack{j=1\\ j\neq i}}^{N}\alpha_j\beta_i\beta_j u_0^m(x_j)\int_{B_{\varepsilon_i}(x_i)} p^\varepsilon_{j\,|_{\Omega\setminus\overline{B_{\varepsilon_j}}}} v^m$$

$$-2k^2\sum_{m=1}^{M}\sum_{i=1}^{N}\sum_{\substack{j=1\\ j\neq i}}^{N}\alpha_i\alpha_j\lambda_3^{\varepsilon_j}\beta_i\beta_j u_0^m(x_j)\,v^m(x_i)\,q_j(x_i)$$

$$+k^2\sum_{m=1}^{M}\sum_{i=1}^{N}\sum_{j=1}^{N}\alpha_i\alpha_j\lambda_3^{\varepsilon_i}\lambda_3^{\varepsilon_j}\beta_i\beta_j u_0^m(x_i)\,u_0^m(x_j)\,\mathcal{I}_{ij} + \sum_{m=1}^{M}\sum_{\ell=1}^{15}\mathcal{E}_\ell^m(\varepsilon), \quad \text{(A.19)}$$

with

$$\mathcal{I}^{\varepsilon_i} = \int_{B_{\varepsilon_i}(x_i)} I_0(\sqrt{k}\|x - x_i\|), \tag{A.20}$$

and $\mathcal{I}_{ij}$ given by (4.7). The new remainders are such that

$$\mathcal{E}_{11}^{m}(\varepsilon) = -2k^2 \sum_{i=1}^{N} \alpha_i \beta_i^2 u_0^m(x_i) \int_{B_{\varepsilon_i}(x_i)} h_{i\,|B_{\varepsilon_i}}^{\varepsilon} \left(v^m - v^m(x_i)\right), \tag{A.21}$$

$$\mathcal{E}_{12}^{m}(\varepsilon) = -2k^2 \sum_{i=1}^{N} \alpha_i \lambda_3^{\varepsilon_i} \beta_i^2 u_0^m(x_i)\, v^m(x_i) \int_{B_{\varepsilon_i}(x_i)} \left(q_i - q_i(x_i)\right), \tag{A.22}$$

$$\mathcal{E}_{13}^{m}(\varepsilon) = -2k^2 \sum_{i=1}^{N} \sum_{\substack{j=1 \\ j\neq i}}^{N} \alpha_j \lambda_3^{\varepsilon_j} \beta_i \beta_j u_0^m(x_j)\, q_j(x_i) \int_{B_{\varepsilon_i}(x_i)} \left(v^m - v^m(x_i)\right), \tag{A.23}$$

$$\mathcal{E}_{14}^{m}(\varepsilon) = -2k^2 \sum_{i=1}^{N} \sum_{\substack{j=1 \\ j\neq i}}^{N} \alpha_j \lambda_3^{\varepsilon_j} \beta_i \beta_j u_0^m(x_j)\, v^m(x_i) \int_{B_{\varepsilon_i}(x_i)} \left(q_j - q_j(x_i)\right), \tag{A.24}$$

$$\mathcal{E}_{15}^{m}(\varepsilon) = -2k^2 \sum_{i=1}^{N} \sum_{\substack{j=1 \\ j\neq i}}^{N} \alpha_j \lambda_3^{\varepsilon_j} \beta_i \beta_j u_0^m(x_j) \int_{B_{\varepsilon_i}(x_i)} \left(q_j - q_j(x_i)\right)\left(v^m - v^m(x_i)\right). \tag{A.25}$$

Now, let us obtain an explicit form depending on ε_i for $\mathcal{I}^{\varepsilon_i}$. From (A.20), the integral gives us

$$\mathcal{I}^{\varepsilon_i} = \frac{2\pi}{\sqrt{k}} \varepsilon_i I_1(\sqrt{k}\varepsilon_i) = \pi\varepsilon_i^2 + \frac{1}{8}k\pi\varepsilon_i^4 + \tilde{\mathcal{I}}^{\varepsilon_i} \tag{A.26}$$

with $\tilde{\mathcal{I}}^{\varepsilon_i} = O(\varepsilon_i^6)$, where we have used the asymptotic expansion (2.7) of the function $I_1(\sqrt{k}\varepsilon_i)$.

We can simplify (A.19) further by noting the following:

(i) In the first and fifth terms on the right-hand side of (A.19), we can consider the Taylor's expansions of the functions u_0^m, v^m and $p_{j\,|\Omega\setminus\overline{B_{\varepsilon_j}}}^{\varepsilon}$ around the point x_i, namely,

$$u_0^m(x) = u_0^m(x_i) + \nabla u_0^m(x_i)\cdot(x - x_i) + \frac{1}{2}\nabla^2 u_0^m(x_i)(x - x_i)\cdot(x - x_i) + D^3 u_0^m(\widehat{x})(x - x_i)^3, \tag{A.27}$$

$$v^m(x) = v^m(x_i) + \nabla v^m(x_i)\cdot(x - x_i) + \frac{1}{2}\nabla^2 v^m(x_i)(x - x_i)\cdot(x - x_i) + D^3 v^m(\widehat{x})(x - x_i)^3, \tag{A.28}$$

and

$$p^{\varepsilon}_{j|_{\Omega\setminus\overline{B_{\varepsilon_j}}}}(x) \;=\; p^{\varepsilon}_{j|_{\Omega\setminus\overline{B_{\varepsilon_j}}}}(x_i) + \nabla p^{\varepsilon}_{j|_{\Omega\setminus\overline{B_{\varepsilon_j}}}}(x_i)\cdot(x-x_i) + D^2 p^{\varepsilon}_{j|_{\Omega\setminus\overline{B_{\varepsilon_j}}}}(\widehat{x})\,(x-x_i)^2\,, \tag{A.29}$$

respectively, where $\widehat{x}$ is an intermediate point between x and x_i. Moreover, $D^n f(\widehat{x})(x-x_i)^n$, $n \geq 1$, $n \in \mathbb{N}$, denotes the last nth term of the Taylor's expansion of a function $f(x)$ around x_i. Since the function $p^{\varepsilon}_{j|_{\Omega\setminus\overline{B_{\varepsilon_j}}}}$ is written in terms of $\lambda_3^{\varepsilon_j}$, we also use the asymptotic expansion (3.24) in further calculations related to the fifth integral.

(ii) In all other terms of (A.19), we simply use the asymptotic expansions of $\lambda_1^{\varepsilon_i}$, $\lambda_2^{\varepsilon_i}$, $\lambda_3^{\varepsilon_i}$ and $\mathcal{I}^{\varepsilon_i}$ given by (3.19), (3.22), (3.24) and (A.26), respectively.

Finally, after taking into account the above mentioned observations, (A.19) takes the form

$$\begin{aligned}
\mathcal{J}_\varepsilon(u_\varepsilon) - \mathcal{J}_0(u_0) = &-2k\sum_{m=1}^{M}\sum_{i=1}^{N}\alpha_i\beta_i u_0^m(x_i)\,v^m(x_i) - \frac{1}{2\pi}k^2\sum_{m=1}^{M}\sum_{i=1}^{N}\alpha_i^2\ln\alpha_i\;\beta_i^2 u_0^m(x_i)\,v^m(x_i)\\
&-\frac{1}{2\pi}k^2\sum_{m=1}^{M}\sum_{i=1}^{N}\alpha_i^2\beta_i u_0^m(x_i)\,v^m(x_i) - \frac{1}{2\pi}k\sum_{m=1}^{M}\sum_{i=1}^{N}\alpha_i^2\beta_i\nabla u_0^m(x_i)\cdot\nabla v^m(x_i)\\
&-\frac{1}{4\pi}\sigma k^2\sum_{m=1}^{M}\sum_{i=1}^{N}\alpha_i^2\beta_i^2 u_0^m(x_i)\,v^m(x_i) + \frac{1}{\pi}k^2\sum_{m=1}^{M}\sum_{i=1}^{N}\alpha_i^2\beta_i^2 u_0^m(x_i)\,v^m(x_i)\,q_i(x_i)\\
&+\frac{1}{\pi}k^2\sum_{m=1}^{M}\sum_{i=1}^{N}\sum_{\substack{j=1\\ j\neq i}}^{N}\alpha_i\alpha_j\beta_i\beta_j u_0^m(x_j)\,v^m(x_i)\,\mathcal{K}_{ij} + \frac{1}{\pi}k^2\sum_{m=1}^{M}\sum_{i=1}^{N}\sum_{\substack{j=1\\ j\neq i}}^{N}\alpha_i\alpha_j\beta_i\beta_j u_0^m(x_j)\,v^m(x_i)\,q_j(x_i)\\
&+\frac{1}{4\pi^2}k^2\sum_{m=1}^{M}\sum_{i=1}^{N}\sum_{j=1}^{N}\alpha_i\alpha_j\beta_i\beta_j u_0^m(x_i)\,u_0^m(x_j)\,\mathcal{I}_{ij} + \mathcal{E}(\varepsilon) + \mathcal{R}(\varepsilon),
\end{aligned} \tag{A.30}$$

where σ is a constant independent of ε_i given by (4.5) and $\mathcal{K}_{ij}$ is given by (4.6). Moreover, we have

$$\mathcal{E}(\varepsilon) = \sum_{m=1}^{M}\sum_{\ell=1}^{23}\mathcal{E}_\ell^m(\varepsilon) \qquad \text{and} \qquad \mathcal{R}(\varepsilon) = \sum_{m=1}^{M}\sum_{k=1}^{14}\mathcal{R}_k^m(\varepsilon)\,. \tag{A.31}$$

The new remainders are such that

$$\mathcal{E}_{16}^m(\varepsilon) = -2k\sum_{i=1}^{N}\beta_i\int_{B_{\varepsilon_i}(x_i)}\left[\nabla u_0^m(x_i)\cdot(x-x_i)\right]\left[D^3 v^m(\widehat{x})\,(x-x_i)^3\right], \tag{A.32}$$

$$\mathcal{E}_{17}^m(\varepsilon) = -2k\sum_{i=1}^{N}\beta_i\int_{B_{\varepsilon_i}(x_i)}\left[D^2 u_0^m(x_i)\,(x-x_i)^2\right]\left[D^2 v^m(x_i)\,(x-x_i)^2\right], \tag{A.33}$$

$$\mathcal{E}_{18}^m(\varepsilon) = -2k\sum_{i=1}^{N}\beta_i\int_{B_{\varepsilon_i}(x_i)}\left[\nabla v^m(x_i)\cdot(x-x_i)\right]\left[D^3 u_0^m(\widehat{x})\,(x-x_i)^3\right], \tag{A.34}$$

$$\mathcal{E}_{19}^{m}(\varepsilon) = -2k\sum_{i=1}^{N}\beta_i\int_{B_{\varepsilon_i}(x_i)}\left[D^3u_0^m(\widehat{x})(x-x_i)^3\right]\left[D^3v^m(\widehat{x})(x-x_i)^3\right], \quad \text{(A.35)}$$

$$\mathcal{E}_{20}^{m}(\varepsilon) = -2k^2\sum_{i=1}^{N}\sum_{\substack{j=1\\ j\neq i}}^{N}\alpha_j\beta_i\beta_j u_0^m(x_j)\, p_{j}^{\varepsilon}{}_{|_{\Omega\setminus\overline{B_{\varepsilon_j}}}}(x_i)\int_{B_{\varepsilon_i}(x_i)}D^2v^m(\widehat{x})(x-x_i)^2, \quad \text{(A.36)}$$

$$\mathcal{E}_{21}^{m}(\varepsilon) = -2k^2\sum_{i=1}^{N}\sum_{\substack{j=1\\ j\neq i}}^{N}\alpha_j\beta_i\beta_j u_0^m(x_j)\, v^m(x_i)\int_{B_{\varepsilon_i}(x_i)}D^2p_{j}^{\varepsilon}{}_{|_{\Omega\setminus\overline{B_{\varepsilon_j}}}}(\widehat{x})(x-x_i)^2, \quad \text{(A.37)}$$

$$\mathcal{E}_{22}^{m}(\varepsilon) = -2k^2\sum_{i=1}^{N}\sum_{\substack{j=1\\ j\neq i}}^{N}\alpha_j\beta_i\beta_j u_0^m(x_j)\int_{B_{\varepsilon_i}(x_i)}[\nabla p_{j}^{\varepsilon}{}_{|_{\Omega\setminus\overline{B_{\varepsilon_j}}}}(x_i)\cdot(x-x_i)][\nabla v^m(x_i)\cdot(x-x_i)], \quad \text{(A.38)}$$

$$\mathcal{E}_{23}^{m}(\varepsilon) = -2k^2\sum_{i=1}^{N}\sum_{\substack{j=1\\ j\neq i}}^{N}\alpha_j\beta_i\beta_j u_0^m(x_j)\int_{B_{\varepsilon_i}(x_i)}[D^2p_{j}^{\varepsilon}{}_{|_{\Omega\setminus\overline{B_{\varepsilon_j}}}}(\widehat{x})(x-x_i)^2][D^2v^m(\widehat{x})(x-x_i)^2]. \quad \text{(A.39)}$$

Additionally, the use of the asymptotic expansions of $\lambda_1^{\varepsilon_i}$, $\lambda_2^{\varepsilon_i}$, $\lambda_3^{\varepsilon_i}$ and $\mathcal{I}^{\varepsilon_i}$ in (A.19) produces residual terms, namely,

$$\mathcal{R}_{1}^{m}(\varepsilon) = -2k\sum_{i=1}^{N}\tilde{\mathcal{I}}^{\varepsilon_i}\beta_i^2u_0^m(x_i)\,v^m(x_i) = O(|\varepsilon|^6), \quad \text{(A.40)}$$

$$\mathcal{R}_{2}^{m}(\varepsilon) = -\frac{1}{4}k^3\pi^2\lambda\sum_{i=1}^{N}\varepsilon_i^6\beta_i^2u_0^m(x_i)\,v^m(x_i) = O(|\varepsilon|^6), \quad \text{(A.41)}$$

$$\mathcal{R}_{3}^{m}(\varepsilon) = -2k^2\pi\lambda\sum_{i=1}^{N}\varepsilon_i^2\tilde{\mathcal{I}}^{\varepsilon_i}\beta_i^2u_0^m(x_i)\,v^m(x_i) = O(|\varepsilon|^8), \quad \text{(A.42)}$$

$$\mathcal{R}_{4}^{m}(\varepsilon) = -\frac{1}{8}k^3\pi\sum_{i=1}^{N}\varepsilon_i^6\ln\varepsilon_i\;\beta_i^2u_0^m(x_i)\,v^m(x_i) = o(|\varepsilon|^5), \quad \text{(A.43)}$$

$$\mathcal{R}_{5}^{m}(\varepsilon) = -k^2\sum_{i=1}^{N}\varepsilon_i^2\ln\varepsilon_i\;\tilde{\mathcal{I}}^{\varepsilon_i}\beta_i^2u_0^m(x_i)\,v^m(x_i) = o(|\varepsilon|^7), \quad \text{(A.44)}$$

$$\mathcal{R}_{6}^{m}(\varepsilon) = -2k^2\pi^2\sum_{i=1}^{N}\varepsilon_i^4\tilde{\lambda}_2^{\varepsilon_i}\beta_i^2u_0^m(x_i)\,v^m(x_i) = O(|\varepsilon|^6), \quad \text{(A.45)}$$

$$\mathcal{R}_{7}^{m}(\varepsilon) = -\frac{1}{4}k^3\pi^2\sum_{i=1}^{N}\varepsilon_i^6\tilde{\lambda}_2^{\varepsilon_i}\beta_i^2u_0^m(x_i)\,v^m(x_i) = O(|\varepsilon|^8), \quad \text{(A.46)}$$

$$\mathcal{R}_8^m(\varepsilon) = -2k^2\pi \sum_{i=1}^{N} \varepsilon_i^2 \tilde{\lambda}_2^{\varepsilon_i} \tilde{\mathcal{I}}^{\varepsilon_i} \beta_i^2 u_0^m(x_i)\, v^m(x_i) = O(|\varepsilon|^{10}), \tag{A.47}$$

$$\mathcal{R}_9^m(\varepsilon) = -2k^2\pi^2 \sum_{i=1}^{N} \varepsilon_i^4 \tilde{\lambda}_3^{\varepsilon_i} \beta_i^2 u_0^m(x_i)\, v^m(x_i)\, q_i(x_i) = O(|\varepsilon|^{6}), \tag{A.48}$$

$$\mathcal{R}_{10}^m(\varepsilon) = -2k^2\pi^2 \sum_{i=1}^{N} \sum_{\substack{j=1\\ j\neq i}}^{N} \varepsilon_i^2 \varepsilon_j^2 \tilde{\lambda}_3^{\varepsilon_j} \beta_i\beta_j u_0^m(x_j)\, v^m(x_i)\, \mathcal{K}_{ij} = O(|\varepsilon|^{6}), \tag{A.49}$$

$$\mathcal{R}_{11}^m(\varepsilon) = -2k^2\pi^2 \sum_{i=1}^{N} \sum_{\substack{j=1\\ j\neq i}}^{N} \varepsilon_i^2 \varepsilon_j^2 \tilde{\lambda}_3^{\varepsilon_j} \beta_i\beta_j u_0^m(x_j)\, v^m(x_i)\, q_j(x_i) = O(|\varepsilon|^{6}), \tag{A.50}$$

$$\mathcal{R}_{12}^m(\varepsilon) = -\frac{1}{2}k^2\pi \sum_{i=1}^{N} \sum_{j=1}^{N} \varepsilon_i^2 \varepsilon_j^2 \tilde{\lambda}_3^{\varepsilon_j} \beta_i\beta_j u_0^m(x_i)\, u_0^m(x_j)\, \mathcal{I}_{ij} = O(|\varepsilon|^{6}), \tag{A.51}$$

$$\mathcal{R}_{13}^m(\varepsilon) = -\frac{1}{2}k^2\pi \sum_{i=1}^{N} \sum_{j=1}^{N} \varepsilon_i^2 \varepsilon_j^2 \tilde{\lambda}_3^{\varepsilon_i} \beta_i\beta_j u_0^m(x_i)\, u_0^m(x_j)\, \mathcal{I}_{ij} = O(|\varepsilon|^{6}), \tag{A.52}$$

$$\mathcal{R}_{14}^m(\varepsilon) = k^2\pi^2 \sum_{i=1}^{N} \sum_{j=1}^{N} \varepsilon_i^2 \varepsilon_j^2 \tilde{\lambda}_3^{\varepsilon_i} \tilde{\lambda}_3^{\varepsilon_j} \beta_i\beta_j u_0^m(x_i)\, u_0^m(x_j)\, \mathcal{I}_{ij} = O(|\varepsilon|^{8}), \tag{A.53}$$

with $|\varepsilon| = \varepsilon_1 + \cdots + \varepsilon_N$, where the estimates above were obtained taking into account that $\tilde{\lambda}_2^{\varepsilon_i} = O(\varepsilon_i^2)$, $\tilde{\lambda}_3^{\varepsilon_i} = O(\varepsilon_i^2)$ and $\tilde{\mathcal{I}}^{\varepsilon_i} = O(\varepsilon_i^6)$. From (A.40)-(A.53), we conclude that

$$\mathcal{R}(\varepsilon) = \sum_{m=1}^{M} \sum_{k=1}^{14} \mathcal{R}_k^m(\varepsilon) = o(|\varepsilon|^5). \tag{A.54}$$

A.2. **Preliminary lemmas.** In order to simplify the presentation, we denote all the constants independent of ε, i and m as C for $i = 1, \cdots, N$ and $m = 1, \cdots, M$, whose value changes according to the place it is used.

Lemma 2. *For $i = 1, \cdots, N$ and $m = 1, \cdots, M$, let $\tilde{h}_i^{\varepsilon,m}$ be the weak solution of the variational problem to find $\tilde{h}_i^{\varepsilon,m} \in H^1(\Omega)$ such that*

$$\int_\Omega \nabla \tilde{h}_i^{\varepsilon,m} \cdot \nabla \eta + k \int_\Omega \tilde{h}_i^{\varepsilon,m} \eta = -\frac{1}{|B_{\varepsilon_i}(x_i)|} \int_{B_{\varepsilon_i}(x_i)} (u_0^m - u_0^m(x_i))\eta, \ \forall \eta \in H^1(\Omega). \tag{A.55}$$

Then, there exists a positive constant C independent of ε such that

$$\|\tilde{h}_i^{\varepsilon,m}\|_{H^1(\Omega)} \leq C\varepsilon_i^{\delta_i}, \quad \forall i = 1, \cdots, N \quad \textit{and} \quad m = 1, \cdots, M, \tag{A.56}$$

for any $0 < \delta_i < 1$.

Proof. By taking $\eta = \tilde{h}_i^{\varepsilon,m}$ as a test function in (A.55), we have

$$\int_\Omega |\nabla \tilde{h}_i^{\varepsilon,m}|^2 + k\int_\Omega |\tilde{h}_i^{\varepsilon,m}|^2 = -\frac{1}{|B_{\varepsilon_i}(x_i)|}\int_{B_{\varepsilon_i}(x_i)} (u_0^m - u_0^m(x_i))\tilde{h}_i^{\varepsilon,m}. \tag{A.57}$$

From the Cauchy-Schwarz inequality and the interior elliptic regularity of the function u_0^m, there exists a positive constant C independent of ε, i and m such that

$$\begin{aligned}\int_\Omega |\nabla \tilde{h}_i^{\varepsilon,m}|^2 + k\int_\Omega |\tilde{h}_i^{\varepsilon,m}|^2 &\leq C\varepsilon_i^{-2}\|u_0^m - u_0^m(x_i)\|_{L^2(B_{\varepsilon_i})}\|\tilde{h}_i^{\varepsilon,m}\|_{L^2(B_{\varepsilon_i})}\\ &\leq C\varepsilon_i^{-2}\|x - x_i\|_{L^2(B_{\varepsilon_i})}\|\tilde{h}_i^{\varepsilon,m}\|_{L^2(B_{\varepsilon_i})}\\ &\leq C\|\tilde{h}_i^{\varepsilon,m}\|_{L^2(B_{\varepsilon_i})}. \end{aligned}\tag{A.58}$$

Notice that, Hölder inequality and the Sobolev embedding theorem can be used to derive

$$\|\tilde{h}_i^{\varepsilon,m}\|_{L^2(B_{\varepsilon_i})} \leq C\varepsilon_i^{1/q}\|\tilde{h}_i^{\varepsilon,m}\|_{L^{2p}(B_{\varepsilon_i})} \leq C\varepsilon_i^{\delta_i}\|\tilde{h}_i^{\varepsilon,m}\|_{H^1(\Omega)}, \tag{A.59}$$

for any $1 < q < \infty$ with $1/p + 1/q = 1$. Let us denote $\delta_i = 1/q$ which implies $0 < \delta_i < 1$. Using (A.59) in (A.58), we get

$$\int_\Omega |\nabla \tilde{h}_i^{\varepsilon,m}|^2 + k\int_\Omega |\tilde{h}_i^{\varepsilon,m}|^2 \leq C\varepsilon_i^{\delta_i}\|\tilde{h}_i^{\varepsilon,m}\|_{H^1(\Omega)}. \tag{A.60}$$

Hence the fact. □

Corollary 3. *For $i, j = 1, \cdots, N$ and $m = 1, \cdots, M$, let $\tilde{h}_i^{\varepsilon,m}$ be the weak solution of* (A.55)*. Then, there exists a positive constant C independent of ε such that*

$$\|\tilde{h}_i^{\varepsilon,m}\|_{L^2(B_{\varepsilon_j})} \leq C\varepsilon_i^{\delta_i}\varepsilon_j^{\delta_j}, \quad \forall i, j = 1, \cdots, N \quad \text{and} \quad m = 1, \cdots, M, \tag{A.61}$$

for any $0 < \delta_i, \delta_j < 1$.

Proof. Similar to (A.59), from Hölder inequality and the Sobolev embedding theorem, we get

$$\|\tilde{h}_i^{\varepsilon,m}\|_{L^2(B_{\varepsilon_j})} \leq C\varepsilon_j^{\delta_j}\|\tilde{h}_i^{\varepsilon,m}\|_{H^1(\Omega)} \leq C\varepsilon_j^{\delta_j}\varepsilon_i^{\delta_i}, \tag{A.62}$$

for any $0 < \delta_i, \delta_j < 1$. We obtain the last inequality by using Lemma 2. Hence the fact. □

Lemma 4. *For $i, j = 1, \cdots, N$ and $m = 1, \cdots, M$, let $h_i^{\varepsilon,m}$ be written as* (3.16)*. Then, there exists a positive constant C independent of ε such that*

$$\|h_i^{\varepsilon,m}\|_{L^2(B_{\varepsilon_j})} \leq C(\varepsilon_j|\ln\varepsilon_i| + \varepsilon_j + \varepsilon_i^{\delta_i}\varepsilon_j^{\delta_j}), \tag{A.63}$$

for any $0 < \delta_i, \delta_j < 1$ with $i, j = 1, \cdots, N$ and $m = 1, \cdots, M$.

Proof. From the decomposition (3.16) and the triangular inequality, we have

$$\|h_i^{\varepsilon,m}\|_{L^2(B_{\varepsilon_j})} \leq C\left(\|p_i^\varepsilon\|_{L^2(B_{\varepsilon_j})} + \|q_i^\varepsilon\|_{L^2(B_{\varepsilon_j})} + \|\tilde{h}_i^{\varepsilon,m}\|_{L^2(B_{\varepsilon_j})}\right). \tag{A.64}$$

Since the problem satisfied by p_i^ε can be solved explicitly and its solution is given by (3.18), we can establish the following estimate

$$\|p_i^\varepsilon\|_{L^2(B_{\varepsilon_j})} \leq C\varepsilon_j|\ln\varepsilon_i|. \tag{A.65}$$

The function q_i^ε is such that $q_i^\varepsilon = \lambda_3^{\varepsilon_i} q_i$ with $\lambda_3^{\varepsilon_i}$ given by (3.24). From (3.24) and the interior elliptic regularity of the function q_i, we obtain

$$\|q_i^\varepsilon\|_{L^2(B_{\varepsilon_j})} \leq C\varepsilon_j. \tag{A.66}$$

From the estimates (A.65)-(A.66) and Corollary 3, we get

$$\|h_i^{\varepsilon,m}\|_{L^2(B_{\varepsilon_j})} \leq C(\varepsilon_j|\ln \varepsilon_i| + \varepsilon_j + \varepsilon_i^{\delta_i}\varepsilon_j^{\delta_j}) \tag{A.67}$$

which leads to the required estimate (A.63) for any $0 < \delta_i, \delta_j < 1$ with $i, j = 1, \cdots, N$ and $m = 1, \cdots, M$. □

Lemma 5. *For $i = 1, \cdots, N$ and $m = 1, \cdots, M$, let $h_i^{\varepsilon,m}$ be the weak solution of the variational problem* (A.9)*. Then, there exists a positive constant C independent of ε such that*

$$\|h_i^{\varepsilon,m}\|_{H^1(\Omega)} \leq C(\sqrt{|\ln \varepsilon_i|} + 1 + \varepsilon_i^{\delta_i - 1/2}), \tag{A.68}$$

for any $0 < \delta_i < 1$ with $i = 1, \cdots, N$ and $m = 1, \cdots, M$.

Proof. By taking $\eta = h_i^{\varepsilon,m}$ as a test function in (A.9), we have

$$\int_\Omega |\nabla h_i^{\varepsilon,m}|^2 + k\int_\Omega |h_i^{\varepsilon,m}|^2 = -\frac{1}{|B_{\varepsilon_i}(x_i)|}\int_{B_{\varepsilon_i}(x_i)} u_0^m h_i^{\varepsilon,m}. \tag{A.69}$$

From the Cauchy-Schwarz inequality together with the interior elliptic regularity of the function u_0^m and Lemma 4, we obtain

$$\begin{aligned}\int_\Omega |\nabla h_i^{\varepsilon,m}|^2 + k\int_\Omega |h_i^{\varepsilon,m}|^2 &\leq C\varepsilon_i^{-2}\|u_0^m\|_{L^2(B_{\varepsilon_i})}\|h_i^{\varepsilon,m}\|_{L^2(B_{\varepsilon_i})}\\ &\leq C\varepsilon_i^{-1}\|h_i^{\varepsilon,m}\|_{L^2(B_{\varepsilon_i})}\\ &\leq C(|\ln \varepsilon_i| + 1 + \varepsilon_i^{2\delta_i - 1}).\end{aligned} \tag{A.70}$$

Hence the fact. □

Lemma 6. *For $i, j = 1, \cdots, N$ and $m = 1, \cdots, M$, let $h_{ij}^{\varepsilon,m}$ be the weak solution of the variational problem* (A.10)*. Then, there exists a positive constant C independent of ε such that*

$$\|h_{ij}^{\varepsilon,m}\|_{H^1(\Omega)} \leq C\varepsilon_i^{\delta_i - 1}(|\ln \varepsilon_j| + 1 + \varepsilon_i^{\delta_i - 1}\varepsilon_j^{\delta_j}), \tag{A.71}$$

for any $0 < \delta_i, \delta_j < 1$ with $i, j = 1, \cdots, N$ and $m = 1, \cdots, M$.

Proof. By taking $\eta = h_{ij}^{\varepsilon,m}$ as test a function in (A.10), we have

$$\int_\Omega |\nabla h_{ij}^{\varepsilon,m}|^2 + k\int_\Omega |h_{ij}^{\varepsilon,m}|^2 = -\frac{1}{|B_{\varepsilon_i}(x_i)|}\int_{B_{\varepsilon_i}(x_i)} h_j^{\varepsilon,m} h_{ij}^{\varepsilon,m}. \tag{A.72}$$

From the Cauchy-Schwarz inequality and Lemma 4, we obtain

$$\begin{aligned}\int_\Omega |\nabla h_{ij}^{\varepsilon,m}|^2 + k\int_\Omega |h_{ij}^{\varepsilon,m}|^2 &\leq C\varepsilon_i^{-2}\|h_j^{\varepsilon,m}\|_{L^2(B_{\varepsilon_i})}\|h_{ij}^{\varepsilon,m}\|_{L^2(B_{\varepsilon_i})}\\ &\leq C\varepsilon_i^{-1}(|\ln \varepsilon_j| + 1 + \varepsilon_i^{\delta_i - 1}\varepsilon_j^{\delta_j})\|h_{ij}^{\varepsilon,m}\|_{L^2(B_{\varepsilon_i})}.\end{aligned} \tag{A.73}$$

Notice that, Hölder inequality and the Sobolev embedding theorem can be used to derive

$$\|h_{ij}^{\varepsilon,m}\|_{L^2(B_{\varepsilon_i})} \leq C\varepsilon_i^{1/q}\|h_{ij}^{\varepsilon,m}\|_{L^{2p}(B_{\varepsilon_i})} \leq C\varepsilon_i^{\delta_i}\|h_{ij}^{\varepsilon,m}\|_{H^1(\Omega)}, \tag{A.74}$$

for any $1 < q < \infty$ with $1/p + 1/q = 1$. Like earlier, let us denote $\delta_i = 1/q$ which implies $0 < \delta_i < 1$. Using (A.74) into (A.73), we get

$$\int_\Omega |\nabla h_{ij}^{\varepsilon,m}|^2 + k \int_\Omega |h_{ij}^{\varepsilon,m}|^2 \leq C\varepsilon_i^{\delta_i - 1}(|\ln \varepsilon_j| + 1 + \varepsilon_i^{\delta_i-1}\varepsilon_j^{\delta_j})\|h_{ij}^{\varepsilon,m}\|_{H^1(\Omega)}. \quad \text{(A.75)}$$

Hence the fact. □

Lemma 7. *For $m = 1, \cdots, M$, let $\tilde{u}_\varepsilon^m$ be the weak solution of the variational problem to find $\tilde{u}_\varepsilon^m \in H^1(\Omega)$ such that*

$$\int_\Omega \nabla \tilde{u}_\varepsilon^m \cdot \nabla \eta + k_\varepsilon \int_\Omega \tilde{u}_\varepsilon^m \eta = \int_\Omega \Phi_\varepsilon^m \eta, \quad \forall \eta \in H^1(\Omega), \quad \text{(A.76)}$$

where Φ_ε^m is given by (3.12). Then, there exists a positive constant C independent of ε such that

$$\|\tilde{u}_\varepsilon^m\|_{H^1(\Omega)} \leq C \sum_{i,j,l=1}^{N} \varepsilon_l^{2\delta_l}\varepsilon_i^{\delta_i+1}(\varepsilon_j^2|\ln \varepsilon_j| + \varepsilon_j^2 + \varepsilon_i^{\delta_i-1}\varepsilon_j^{\delta_j+2}), \quad \text{(A.77)}$$

for any $0 < \delta_i, \delta_j, \delta_l < 1$ with $i, j, l = 1, \cdots, N$ and $m = 1, \cdots, M$.

Proof. By taking $\eta = \tilde{u}_\varepsilon^m$ as a test function in (A.76), we have

$$\int_\Omega |\nabla \tilde{u}_\varepsilon^m|^2 + k_\varepsilon \int_\Omega |\tilde{u}_\varepsilon^m|^2 = \int_\Omega \Phi_\varepsilon^m \tilde{u}_\varepsilon^m. \quad \text{(A.78)}$$

From the Cauchy-Scharwz inequality, we obtain

$$\begin{aligned}
\int_\Omega |\nabla \tilde{u}_\varepsilon^m|^2 + k_\varepsilon \int_\Omega |\tilde{u}_\varepsilon^m|^2 &\leq C \sum_{l=1}^{N} \|\tilde{u}_\varepsilon^m\|_{L^2(B_{\varepsilon_l})} \sum_{i=1}^{N}\sum_{j=1}^{N} \varepsilon_i^2\varepsilon_j^2 \|h_{ij}^{\varepsilon,m}\|_{L^2(B_{\varepsilon_l})} \\
&\leq C \sum_{i,j,l=1}^{N} \varepsilon_l^{2\delta_l}\varepsilon_i^2\varepsilon_j^2\|h_{ij}^{\varepsilon,m}\|_{H^1(\Omega)}\|\tilde{u}_\varepsilon^m\|_{H^1(\Omega)} \\
&\leq C \sum_{i,j,l=1}^{N} \varepsilon_l^{2\delta_l}\varepsilon_i^{\delta_i+1}(\varepsilon_j^2|\ln \varepsilon_j| + \varepsilon_j^2 + \varepsilon_i^{\delta_i-1}\varepsilon_j^{\delta_j+2})\|\tilde{u}_\varepsilon^m\|_{H^1(\Omega)},
\end{aligned} \quad \text{(A.79)}$$

where we have used the Hölder inequality and the Sobolev embedding theorem with Lemma 6. Hence the fact. □

A.3. **A priori estimates of the remainders.** We shall prove that $\mathcal{E}_\ell^m(\varepsilon) = o(|\varepsilon|^4)$ for $\ell = 1, \ldots, 23$, where $|\varepsilon| := \varepsilon_1 + \cdots + \varepsilon_N$. For simplicity, we use the symbol C to denote any constant independent of ε. The estimate for the remainders are obtained in two steps. We start by using the Cauchy-Schwarz inequality, then

- for the remainders $\mathcal{E}_\ell^m(\varepsilon)$, $\ell = 1, \ldots, 8$, we use the trace theorem and the appropriate lemmas of Section A.2;
- for the remainders $\mathcal{E}_\ell^m(\varepsilon)$, $\ell = 9, 10$, we use Corollary 3 together with the interior elliptic regularity of the function v^m;
- for the remainders $\mathcal{E}_\ell^m(\varepsilon)$, $\ell = 11, \ldots, 15$, we use the interior elliptic regularity of the functions v^m and q_i together with the fact $\|x - x_i\|_{L^2(B_{\varepsilon_i})}^n = O(|\varepsilon|^{n+1})$, $n \in \mathbb{Z}^+$, and the estimate $\lambda_3^{\varepsilon_i} = O(1)$;

- for the remainders $\mathcal{E}_\ell^m(\varepsilon)$, $\ell = 16,\dots,19$, we simply use the fact $\|x - x_i\|^n_{L^2(B_{\varepsilon_i})} = O(|\varepsilon|^{n+1})$, where $n \in \mathbb{Z}^+$;
- for the remainders $\mathcal{E}_\ell^m(\varepsilon)$, $\ell = 20,\dots,23$, we use the fact $\|x-x_i\|^n_{L^2(B_{\varepsilon_i})} = O(|\varepsilon|^{n+1})$, $n \in \mathbb{Z}^+$, observing that $p^\varepsilon_{j|_{\Omega\setminus\overline{B_{\varepsilon_j}}}}$ is given by (3.18) with $\lambda_3^{\varepsilon_j} = O(1)$.

Proceeding in this way, we obtain

$$|\mathcal{E}_1^m(\varepsilon)| \le C\|\tilde{u}_\varepsilon^m\|_{H^1(\Omega)}\|u_0^m - z^m\|_{H^1(\Omega)} \le C\|\tilde{u}_\varepsilon^m\|_{H^1(\Omega)} = o\left(|\varepsilon|^4\right), \tag{A.80}$$

for any $2/5 < \delta < 1$, where we have used Lemma 7;

$$|\mathcal{E}_2^m(\varepsilon)| \le C|\varepsilon|^6 \sum_{i=1}^N \|h_i^{\varepsilon,m}\|_{H^1(\Omega)} \sum_{j=1}^N\sum_{l=1}^N \|h_{jl}^{\varepsilon,m}\|_{H^1(\Omega)} = o\left(|\varepsilon|^4\right), \tag{A.81}$$

for any $1/8 < \delta < 1$, where we have used Lemmas 5 and 6;

$$|\mathcal{E}_3^m(\varepsilon)| \le C|\varepsilon|^2\|\tilde{u}_\varepsilon^m\|_{H^1(\Omega)} \sum_{i=1}^N \|h_i^{\varepsilon,m}\|_{H^1(\Omega)} = o\left(|\varepsilon|^4\right), \tag{A.82}$$

for any $1/12 < \delta < 1$, where we have used Lemmas 5 and 7;

$$|\mathcal{E}_4^m(\varepsilon)| \le C|\varepsilon|^8 \sum_{i=1}^N\sum_{j=1}^N \|h_{ij}^{\varepsilon,m}\|_{H^1(\Omega)} \sum_{l=1}^N\sum_{p=1}^N \|h_{lp}^{\varepsilon,m}\|_{H^1(\Omega)} = o\left(|\varepsilon|^4\right), \tag{A.83}$$

for any $0 < \delta < 1$, where we have used Lemma 6;

$$|\mathcal{E}_5^m(\varepsilon)| \le C|\varepsilon|^4\|\tilde{u}_\varepsilon^m\|_{H^1(\Omega)} \sum_{i=1}^N\sum_{j=1}^N \|h_{ij}^{\varepsilon,m}\|_{H^1(\Omega)} = o\left(|\varepsilon|^4\right), \tag{A.84}$$

for any $0 < \delta < 1$, where we have used Lemmas 6 and 7;

$$|\mathcal{E}_6^m(\varepsilon)| \le C\|\tilde{u}_\varepsilon^m\|_{H^1(\Omega)}\|\tilde{u}_\varepsilon^m\|_{H^1(\Omega)} = o\left(|\varepsilon|^4\right), \tag{A.85}$$

for any $0 < \delta < 1$, where we have used Lemma 7;

$$\begin{aligned} |\mathcal{E}_7^m(\varepsilon)| &\le C|\varepsilon|^4 \sum_{i=1}^N\sum_{j=1}^N \left[\|h_i^\varepsilon\|_{H^{-1/2}(\partial\Omega)}\|\tilde{h}_j^{\varepsilon,m}\|_{H^{1/2}(\partial\Omega)} + \|h_j^\varepsilon\|_{H^{-1/2}(\partial\Omega)}\|\tilde{h}_i^{\varepsilon,m}\|_{H^{1/2}(\partial\Omega)}\right] \\ &\le C|\varepsilon|^4 \sum_{i=1}^N\sum_{j=1}^N \left[\|h_i^\varepsilon\|_{L^2(\Omega)}\|\tilde{h}_j^{\varepsilon,m}\|_{H^1(\Omega)} + \|h_j^\varepsilon\|_{L^2(\Omega)}\|\tilde{h}_i^{\varepsilon,m}\|_{H^1(\Omega)}\right] = o(|\varepsilon^4|), \end{aligned} \tag{A.86}$$

for any $0 < \delta < 1$, where we have used Lemma 2 and the explicit form of h_i^ε, given by (3.28), in order to establish $\|h_i^\varepsilon\|_{L^2(\Omega)} = O(1)$;

$$|\mathcal{E}_8^m(\varepsilon)| \le C|\varepsilon|^4 \sum_{i=1}^N \|\tilde{h}_i^{\varepsilon,m}\|_{H^1(\Omega)} \sum_{j=1}^N \|\tilde{h}_j^{\varepsilon,m}\|_{H^1(\Omega)} = o\left(|\varepsilon|^4\right), \tag{A.87}$$

for any $0 < \delta < 1$, where we have used Lemma 2;

$$|\mathcal{E}_9^m(\varepsilon)| \leq C|\varepsilon|^2 \sum_{i=1}^N \|\tilde{h}_i^{\varepsilon,m}\|_{L^2(B_{\varepsilon_i})}\|v^m\|_{L^2(B_{\varepsilon_i})} \leq C|\varepsilon|^3 \sum_{i=1}^N \|\tilde{h}_i^{\varepsilon,m}\|_{L^2(B_{\varepsilon_i})} = o\left(|\varepsilon|^4\right), \quad \text{(A.88)}$$

for any $1/2 < \delta < 1$;

$$|\mathcal{E}_{10}^m(\varepsilon)| \leq C|\varepsilon|^2 \sum_{i=1}^N \sum_{\substack{j=1\\j\neq i}}^N \|\tilde{h}_j^{\varepsilon,m}\|_{L^2(B_{\varepsilon_i})}\|v^m\|_{L^2(B_{\varepsilon_i})} \leq C|\varepsilon|^3 \sum_{i=1}^N \sum_{\substack{j=1\\j\neq i}}^N \|\tilde{h}_j^{\varepsilon,m}\|_{L^2(B_{\varepsilon_i})} = o\left(|\varepsilon|^4\right), \quad \text{(A.89)}$$

for any $1/2 < \delta < 1$;

$$\begin{aligned}
|\mathcal{E}_{11}^m(\varepsilon)| &\leq C|\varepsilon|^2 \sum_{i=1}^N \|h^\varepsilon_{i|_{B_{\varepsilon_i}}}\|_{L^2(B_{\varepsilon_i})}\|v^m - v^m(x_i)\|_{L^2(B_{\varepsilon_i})} \\
&\leq C|\varepsilon|^2 \sum_{i=1}^N \|h^\varepsilon_{i|_{B_{\varepsilon_i}}}\|_{L^2(B_{\varepsilon_i})}\|x - x_i\|_{L^2(B_{\varepsilon_i})} \\
&\leq C|\varepsilon|^4 \sum_{i=1}^N \|h^\varepsilon_{i|_{B_{\varepsilon_i}}}\|_{L^2(B_{\varepsilon_i})} = o\left(|\varepsilon|^5\right), \qquad \text{(A.90)}
\end{aligned}$$

where we have used the explicit form of $h^\varepsilon_{i|_{B_{\varepsilon_i}}}$ given by (3.28) to obtain $\|h^\varepsilon_{i|_{B_{\varepsilon_i}}}\|_{L^2(B_{\varepsilon_i})} = O(\varepsilon_i|\ln\varepsilon_i|)$;

$$|\mathcal{E}_{12}^m(\varepsilon)| \leq C|\varepsilon|^2 \sum_{i=1}^N \|q_i - q_i(x_i)\|_{L^2(B_{\varepsilon_i})}\|1\|_{L^2(B_{\varepsilon_i})} \leq C|\varepsilon|^3 \sum_{i=1}^N \|x - x_i\|_{L^2(B_{\varepsilon_i})} = O\left(|\varepsilon|^5\right); \quad \text{(A.91)}$$

$$|\mathcal{E}_{13}^m(\varepsilon)| \leq C|\varepsilon|^2 \sum_{i=1}^N \|v^m - v^m(x_i)\|_{L^2(B_{\varepsilon_i})}\|1\|_{L^2(B_{\varepsilon_i})} \leq C|\varepsilon|^3 \sum_{i=1}^N \|x - x_i\|_{L^2(B_{\varepsilon_i})} = O\left(|\varepsilon|^5\right); \quad \text{(A.92)}$$

$$|\mathcal{E}_{14}^m(\varepsilon)| \leq C|\varepsilon|^2 \sum_{i=1}^N \sum_{\substack{j=1\\j\neq i}}^N \|q_j - q_j(x_i)\|_{L^2(B_{\varepsilon_i})}\|1\|_{L^2(B_{\varepsilon_i})} \leq C|\varepsilon|^3 \sum_{i=1}^N \|x - x_i\|_{L^2(B_{\varepsilon_i})} = O\left(|\varepsilon|^5\right); \quad \text{(A.93)}$$

$$\begin{aligned}
|\mathcal{E}_{15}^m(\varepsilon)| &\leq C|\varepsilon|^2 \sum_{i=1}^N \sum_{\substack{j=1\\j\neq i}}^N \|q_j - q_j(x_i)\|_{L^2(B_{\varepsilon_i})}\|v^m - v^m(x_i)\|_{L^2(B_{\varepsilon_i})} \\
&\leq C|\varepsilon|^2 \sum_{i=1}^N \|x - x_i\|_{L^2(B_{\varepsilon_i})}\|x - x_i\|_{L^2(B_{\varepsilon_i})} = O\left(|\varepsilon|^6\right); \qquad \text{(A.94)}
\end{aligned}$$

$$|\mathcal{E}_{16}^m(\varepsilon)| \leq C \sum_{i=1}^N \|x - x_i\|_{L^2(B_{\varepsilon_i})}\|x - x_i\|^3_{L^2(B_{\varepsilon_i})} = O(|\varepsilon|^6); \qquad \text{(A.95)}$$

$$|\mathcal{E}_{17}^{m}(\varepsilon)| \leq C\sum_{i=1}^{N}\|x-x_i\|_{L^2(B_{\varepsilon_i})}^2\|x-x_i\|_{L^2(B_{\varepsilon_i})}^2 = O(|\varepsilon|^6); \tag{A.96}$$

$$|\mathcal{E}_{18}^{m}(\varepsilon)| \leq C\sum_{i=1}^{N}\|x-x_i\|_{L^2(B_{\varepsilon_i})}\|x-x_i\|_{L^2(B_{\varepsilon_i})}^3 = O(|\varepsilon|^6); \tag{A.97}$$

$$|\mathcal{E}_{19}^{m}(\varepsilon)| \leq C\sum_{i=1}^{N}\|x-x_i\|_{L^2(B_{\varepsilon_i})}^3\|x-x_i\|_{L^2(B_{\varepsilon_i})}^3 = O(|\varepsilon|^8); \tag{A.98}$$

$$|\mathcal{E}_{20}^{m}(\varepsilon)| \leq C|\varepsilon|^2\sum_{i=1}^{N}\|x-x_i\|_{L^2(B_{\varepsilon_i})}^2\|1\|_{L^2(B_{\varepsilon_i})} = O(|\varepsilon|^6); \tag{A.99}$$

$$|\mathcal{E}_{21}^{m}(\varepsilon)| \leq C|\varepsilon|^2\sum_{i=1}^{N}\|x-x_i\|_{L^2(B_{\varepsilon_i})}^2\|1\|_{L^2(B_{\varepsilon_i})} = O(|\varepsilon|^6); \tag{A.100}$$

$$|\mathcal{E}_{22}^{m}(\varepsilon)| \leq C|\varepsilon|^2\sum_{i=1}^{N}\|x-x_i\|_{L^2(B_{\varepsilon_i})}\|x-x_i\|_{L^2(B_{\varepsilon_i})} = O(|\varepsilon|^6); \tag{A.101}$$

$$|\mathcal{E}_{23}^{m}(\varepsilon)| \leq C|\varepsilon|^2\sum_{i=1}^{N}\|x-x_i\|_{L^2(B_{\varepsilon_i})}^2\|x-x_i\|_{L^2(B_{\varepsilon_i})}^2 = O(|\varepsilon|^8). \tag{A.102}$$

From (A.80)-(A.102), we conclude that

$$\mathcal{E}(\varepsilon) = \sum_{m=1}^{M}\sum_{\ell=1}^{23}\mathcal{E}_{\ell}^{m}(\varepsilon) = o\left(|\varepsilon|^4\right). \tag{A.103}$$

References

[1] A. Ben Abda, M. Hassine, M. Jaoua, and M. Masmoudi. Topological sensitivity analysis for the location of small cavities in stokes flow. *SIAM Journal on Control and Optimization*, 48:2871–2900, 2009.

[2] H. Ammari, J. Garnier, W. Jing, H. Kang, M. Lim, K. Sølna, and H. Wang. *Mathematical and statistical methods for multistatic imaging*, volume 2098. Springer, Switzerland, 2013.

[3] H. Ammari, J. Garnier, V. Jugnon, and H. Kang. Stability and resolution analysis for a topological derivative based imaging functional. *SIAM Journal on Control and Optimization*, 50(1):48–76, 2012.

[4] H. Ammari and H. Kang. *Reconstruction of small inhomogeneities from boundary measurements.* Lectures Notes in Mathematics vol. 1846. Springer-Verlag, Berlin, 2004.

[5] S. Amstutz and N. Dominguez. Topological sensitivity analysis in the context of ultrasonic non-destructive testing. *Engineering Analysis with Boundary Elements*, 32(11):936–947, 2008.

[6] S. Amstutz, I. Horchani, and M. Masmoudi. Crack detection by the topological gradient method. *Control and Cybernetics*, 34(1):81–101, 2005.

[7] J. Baumeister and A. Leitão. *Topics in inverse problems.* IMPA Mathematical Publications, Rio de Janeiro, 2005.

[8] M. Bonnet. Topological sensitivity for 3D elastodynamic and acoustic inverse scattering in the time domain. *Computer Methods in Applied Mechanics and Engineering*, 195(37-40):5239–5254, 2006.

[9] M. Bonnet. Higher-order topological sensitivity for 2-D potential problems. *International Journal of Solids and Structures*, 46(11–12):2275–2292, 2009.

[10] M. Burger. A level set method for inverse problems. *Inverse Problems*, 17:1327–1356, 2001.

[11] M. Burger, B. Hackl, and W. Ring. Incorporating topological derivatives into level set methods. *Journal of Computational Physics*, 194(1):344–362, 2004.

[12] A. Canelas, A. Laurain, and A. A. Novotny. A new reconstruction method for the inverse potential problem. *Journal of Computational Physics*, 268:417–431, 2014.

[13] A. Canelas, A. Laurain, and A. A. Novotny. A new reconstruction method for the inverse source problem from partial boundary measurements. *Inverse Problems*, 31(7):075009, 2015.

[14] A. Carpio and M-L. Rapún. Solving inhomogeneous inverse problems by topological derivative methods. *Inverse Problems*, 24(4):045014, 2008.

[15] I. Chikichev and B. B. Guzina. Generalized topological derivative for the navier equation and inverse scattering in the time domain. *Computer Methods in Applied Mechanics and Engineering*, 194:4467–4484, 2008.

[16] K. Doel, U. Ascher, and A. Leitão. Multiple level sets for piecewise constant surface reconstruction in highly ill-posed problems. *Journal of Scientific Computing*, 43:44–66, 2010.

[17] N. Dominguez and V. Gibiat. Non-destructive imaging using the time domain topological energy method. *Ultrasonics*, 50(3):367–372, 2010.

[18] G. R. Feijóo. A new method in inverse scattering based on the topological derivative. *Inverse Problems*, 20(6):1819–1840, 2004.

[19] L. Fernandez, A. A. Novotny, and R. Prakash. Noniterative reconstruction method for an inverse potential problem modeled by a modified Helmholtz equation. *Numerical Functional Analysis and Optimization*, 39(9):937–966, 2018. DOI: 10.1080/01630563.2018.1432645.

[20] L. Fernandez, A. A. Novotny, and R. Prakash. Topological asymptotic analysis of an optimal control problem modeled by a coupled system. *Asymptotic Analysis*, 109(1–2):1–26, 2018. DOI: 10.3233/ASY-181465.

[21] A.D. Ferreira and A. A. Novotny. A new non-iterative reconstruction method for the electrical impedance tomography problem. *Inverse Problems*, 33(3):035005, 2017.

[22] J. F. Funes, J. M. Perales, M. L. Rapún, and J. M. Manuel Vega. Defect detection from multi-frequency limited data via topological sensitivity. *Journal of Mathematical Imaging and Vision*, 55:19–35, 2016.

[23] B. B. Guzina and M. Bonnet. Small-inclusion asymptotic of misfit functionals for inverse problems in acoustics. *Inverse Problems*, 22(5):1761–1785, 2006.

[24] B. B. Guzina and F. Pourahmadian. Why the high-frequency inverse scattering by topological sensitivity may work. *Proceeding of the Royal Society A: Mathematical, Physical and Engineering Sciences*, 471(2179):20150187, 2015.

[25] M. Hintermüller and A. Laurain. Electrical impedance tomography: from topology to shape. *Control and Cybernetics*, 37(4):913–933, 2008.

[26] M. Hintermüller, A. Laurain, and A. A. Novotny. Second-order topological expansion for electrical impedance tomography. *Advances in Computational Mathematics*, 36(2):235–265, 2012.

[27] V. Isakov. *Inverse problems for partial differential equations.* Applied Mathematical Sciences vol. 127. Springer, New York, 2006.

[28] V. Isakov, S. Leung, and J. Qian. A fast local level set method for inverse gravimetry. *Communications in Computational Physics*, 10(4):1044–1070, 2011.

[29] A. Jeffrey. *Handbook of mathematical formulas and integrals.* Elsevier Academic Press, Amsterdam, Boston, 3rd edition, 2004.

[30] M. Jleli, B. Samet, and G. Vial. Topological sensitivity analysis for the modified Helmholtz equation under an impedance condition on the boundary of a hole. *Journal de Mathématiques Pures et Appliquées*, 103:557–574, 2015.

[31] A. Kirsch. *An introduction to the mathematical theory of inverse problems*, volume 120 of *Applied Mathematical Sciences*. Springer-Verlag, New York, 1996.

[32] V. A. Kovtunenko and K. Kunisch. High precision identification of an object: optimality-conditions-based concept of imaging. *SIAM Journal on Control and Optimization*, 52(1):773–796, 2014.

[33] T. J. Machado, J. S. Angelo, and A. A. Novotny. A new one-shot pointwise source reconstruction method. *Mathematical Methods in the Applied Sciences*, 40(15):1367–1381, 2017.

[34] A. A. Novotny and J. Sokołowski. *Topological derivatives in shape optimization*. Interaction of Mechanics and Mathematics. Springer-Verlag, Berlin, Heidelberg, 2013.
[35] S. S. Rocha and A. A. Novotny. Obstacles reconstruction from partial boundary measurements based on the topological derivative concept. *Structural and Multidisciplinary Optimization*, 55(6):2131–2141, 2017.
[36] B. Samet, S. Amstutz, and M. Masmoudi. The topological asymptotic for the Helmholtz equation. *SIAM Journal on Control and Optimization*, 42(5):1523–1544, 2003.
[37] J. Sokołowski and A. Żochowski. On the topological derivative in shape optimization. *SIAM Journal on Control and Optimization*, 37(4):1251–1272, 1999.
[38] R. Tokmashev, A. Tixier, and B. B. Guzina. Experimental validation of the topological sensitivity approach to elastic-wave imaging. *Inverse Problems*, 29:125005, 2013.
[39] P. Tricarico. Global gravity inversion of bodies with arbitrary shape. *Geophysical Journal International*, 195(1):260–275, 2013.

(L. Fernandez) Laboratório Nacional de Computação Científica LNCC/MCT, Coordenação de Matemática Aplicada e Computacional, Av. Getúlio Vargas 333, 25651-075 Petrópolis - RJ, Brasil
E-mail address: lucasf@lncc.br

(A.A. Novotny) Laboratório Nacional de Computação Científica LNCC/MCT, Coordenação de Matemática Aplicada e Computacional, Av. Getúlio Vargas 333, 25651-075 Petrópolis - RJ, Brasil
E-mail address: novotny@lncc.br

(R. Prakash) Department of Mathematics, Faculty of Physical Science and Mathematics, University of Concepcion, Concepcion, Chile
E-mail address: rprakash@udec.cl